

NACA RM L53B16

7407



RESEARCH MEMORANDUM

EFFECTS OF SLOT SIZE AND GEOMETRY ON THE
FLOW IN RECTANGULAR TUNNELS AT
MACH NUMBERS UP TO 1.4

By William J. Nelson and James M. Cabbage, Jr.

Langley Aeronautical Laboratory
Langley Field, Va.

NATIONAL ADVISORY COMMITTEE
FOR AERONAUTICS

WASHINGTON
April 7, 1953
Declassified March 18, 1957

4-5-53



M NACA RM L53B16

NATIONAL ADVISORY COMMITTEE FOR AERONAUTICS

RESEARCH MEMORANDUM

EFFECTS OF SLOT SIZE AND GEOMETRY ON THE
FLOW IN RECTANGULAR TUNNELS AT
MACH NUMBERS UP TO 1.4

By William J. Nelson and James M. Cabbage, Jr.

SUMMARY

An investigation has been made of the effects of slot width, depth, shape, and spacing on the center-line pressure distribution in rectangular tunnels of constant cross section with several height-to-width ratios. Results are presented in the form of center-line static-pressure distributions and calculated static-pressure and angle-of-flow distributions along the slotted boundary. The latter was accomplished by the method of characteristics using the center-line pressure distribution as a starting point and assuming isentropic flow throughout the length of the tunnel. The data show that transonic flows with a maximum deviation in Mach number less than ± 0.01 can be generated in a rectangular tunnel with fixed-geometry slots for Mach numbers up to 1.4, the limit of the tests. It is also shown that changes in the effective free area ratio of the boundary and in the length of the tapered slot opening cause large changes in axial pressure distribution. With a given slot configuration more uniform flows were obtained in tunnels of large height-width ratio.

INTRODUCTION

The feasibility of generating supersonic Mach numbers by the controlled removal of air from a slotted channel of constant cross section is well-established, references 1 to 5, and many slotted tunnels are now operating in the transonic regime. The design of such facilities, however, frequently requires extensive calibration and modification to establish uniform flow throughout a short test section, and the final slot configurations vary markedly from one tunnel to another. A series of tests has been made in rectangular tunnels of various height-to-width ratios at the Internal Aerodynamics Branch of the Langley Laboratory

to determine the effect of several slot parameters on the Mach number distribution along the test section. Although the range of variables covered is small, it is sufficient to permit explanation of many of the conflicting results obtained in independent tests and, when used as a guide in the development of final slot shape for transonic facilities, should reduce the necessary development work. In these tests, Mach numbers up to 1.4 have been obtained. Data are presented in the form of static-pressure distributions measured along the channel center line and pressure and mean-angle-of-flow distribution along the slotted wall; the flow along the slotted wall was established by the method of characteristics using the measured center-line pressure as a starting point with the assumption of two-dimensional flow along the channel and uniform velocity at the entrance to the slotted region.

SYMBOLS

d_s	depth of slot, in.
h	effective height of channel, in.
L	length of slot taper, in.
M	Mach number corresponding to p/P_0
M_c	Mach number corresponding to p_c/P_0
n	number of slots in each slotted wall
P_0	stagnation pressure
p	local static pressure along channel center line
p_w	local static pressure along slotted wall
p_c	chamber static pressure
w	width of channel, in.
w_s	width of slot, in.
w_{sx}	width of slot at any point x , in.
x	distance along channel measured from upstream end of slot, in.
ϕ	slot taper included angle

- θ_w angle of flow relative to wall; positive towards wall
- ν flow deviation angle from direction at $M = 1.0$

APPARATUS

The general arrangement of the experimental apparatus used in this investigation is presented in figure 1(a). The channels tested were $4\frac{1}{2}$ inches high but differed in width from $2\frac{1}{4}$ inches to $6\frac{1}{4}$ inches; the cross section was constant for approximately 17 inches. In several of the configurations tested a reflection plane was installed, in place of a slotted wall, in the top boundary of the channel, thus producing a channel with an effective height twice its physical height. The dimensions of the plenum chamber surrounding the channel were large relative to those of the channel. The pressure within this chamber was regulated by adjustment of a remotely controlled vacuum system whose operation was completely independent of the main-stream power.

The slotted boundaries were built up from brass bars, the number and shape varying for the different channel widths and slot configurations tested. All slot configurations reported herein were placed in both the top and bottom walls of the channels except when use was made of the reflection plane. Pertinent dimensions of all slot configurations tested are given in table I. A 0.025-inch gap between the slotted wall and the side walls was used in the single slot configuration of the $6\frac{1}{4}$ -inch-wide channel and all configurations tested in the $2\frac{1}{4}$ -inch-wide channel; this gap was added to the value of nw_s in computing the free area of the boundary for those configurations. Figure 1(b) shows the channel and plenum-chamber assembly and in figure 1(c) the $4\frac{1}{2}$ -by $6\frac{1}{4}$ -inch channel configuration is shown. Figure 1(d) shows assembly of the channel and best slot configuration tested for the $4\frac{1}{2}$ -by $4\frac{1}{2}$ -inch channel. The variation of the ratio of the open width to the total width of the slotted boundary with the distance from the upstream end of the slot is presented in figure 2 for all tapered slot configurations tested.

Center-line static pressures were measured by a remotely controlled, 0.060-inch-diameter, static probe having four static orifices 0.0135 inch in diameter located 0.660 inch behind the base of the $6\frac{1}{2}^\circ$ conical tip. The maximum length of travel for the probe was $11\frac{1}{2}$ inches and its zero position was set in the plane of the slot origin. Center-line static pressures for the reflection-plane configurations were measured by

0.030-inch-diameter orifices spaced at 1/2-inch intervals along the reflection-plane surface. Stagnation pressures and temperatures were measured upstream of the entrance bell. Moisture condensation was avoided by operating at stagnation temperatures up to 250° F; the corresponding stagnation pressure was of the order of 2 atmospheres. Stagnation pressures, probe static pressures, and chamber static pressures were read from mercury-filled U-tube manometers. Static pressures from the reflection plane were recorded photographically from a multitube manometer board.

RESULTS

The axial pressure distribution through each of the tunnel configurations investigated is presented for various chamber pressure ratios p_c/P_0 in figures 3 to 6. The data presented in figures 3 and 4 were taken in $2\frac{1}{4}$ -by- $4\frac{1}{2}$ -inch and $6\frac{1}{4}$ -by- $4\frac{1}{2}$ -inch channels with a reflection plane opposite the slotted wall giving channels whose effective height was 9 inches. The pressure distributions obtained in a $6\frac{1}{4}$ -by- $4\frac{1}{2}$ -inch channel with rectangular slots of constant depth in opposite walls are presented in figures 5(a) to (c) and for slots with tapered plan form in figures 5(d) to (h). The data of figure 6(a) were obtained with widely separated tapered slots in opposite walls of a $4\frac{1}{2}$ -inch-square channel and in figure 6(b) the same plan form was used in slots also tapered in depth.

These results show a generally smooth initial expansion followed by a more or less variable pressure as the static pressure in the tunnel approaches that in the chamber. The Mach number attainable in a given channel is shown to increase as the chamber pressure ratio is reduced and the maximum Mach number attainable is shown to increase with the free area of the boundary. In some configurations tapered slots were found to produce more uniform pressure than rectangular slots and in other configurations the reverse was true. Slots tapered in width and depth were found to produce very uniform pressure along the axis of a square tunnel throughout the Mach number range of these tests, that is, to $M = 1.4$.

DISCUSSION

In analyzing the data presented in figures 3 to 6, it is desirable to examine the pressure variations and the angle of flow along the

slotted wall. As a basis for such comparisons the flows in a free jet and in a minimum-length nozzle have been calculated for a single Mach number ($M = 1.2$) by the method of characteristics; these are presented in figure 7. The numbers that appear in the characteristic networks of figure 7(a) are values of the calculated flow angle deviation from $M = 1.0$. The external pressure ratio for the free jet is identical to the final pressure ratio in the minimum-length nozzle; hence, the flow from the free jet turns immediately to the value of v corresponding to that pressure ratio while the flow at the inlet of the minimum-length nozzle turns only $v/2$. The curves of θ_w and p_w/P_0 plotted against x of figure 7(b) show the pressure and flow-angle distribution that would occur along the position for a slotted boundary placed in these flows as indicated in figure 7(a). It is noted that one complete cycle for the free-jet expansion is not shown in figure 7(a); all of the compression waves reflect to one point, from which point the jet repeats the cycle of overexpansion and then overcompression indefinitely. Along the center line of the free jet, pressures substantially below the chamber pressure result from the cumulative effects of expansion at both the upper and lower boundaries; an initial expansion to sub-chamber pressures will therefore in a slotted tunnel indicate excessive slot area. The uniform rapid expansion to the design Mach number in the minimum-length nozzle represents an optimum design.

Effect of channel height-width ratio.- Data obtained in tests of three channel configurations with 1/5-open boundaries and slots of approximately the same geometry ($w_s = 0.057$ to 0.066 inch and $d_s = 1/2$ inch) have been presented in figures 3, 4, and 5(b). Aerodynamically these slots are considered comparable, that is, equal pressure differences across the slots would result in equal flow rates through them. Comparison of the results of figures 3, 4, and 5(b), however, shows substantial differences in center-line pressures for comparable chamber pressure ratios. The initial rate of expansion appears essentially constant for all three configurations; the extent of this expansion, however, is in general shown to decrease as the height-width ratio of the channel increases. With increasing height-width ratio, the pressure variations along the channel are also reduced. A qualitative explanation of these differences can be found in an examination of the effect of the boundary-layer growth along the channel walls.

In closed channels it is common practice to diverge the walls an amount equal to the growth in the displacement thickness of the boundary layer. In a slotted channel of constant cross-sectional area, this effect must be accomplished by removal of air through the slots. The amount of air to be removed in the latter case is approximately equal to the increase in boundary-layer displacement thickness times channel

periphery $2(h + w)\Delta\delta^*$. With the slot area equal to $\left(\frac{nw_s}{w}\right)w$ per wall, it is apparent that for constant $\Delta\delta^*$ the rate at which air must flow through the slots increases as h/w increases. With identical rates of flow through the slots, that part of the flow necessary to overcome the effects of the boundary layer is a greater proportion of the total flow in channels of larger h/w ; thus, for equal chamber pressure ratios, less supersonic expansion occurs in these channels. It is thus apparent that data obtained in tests of rectangular channels with slotted or porous walls cannot be applied to the design of facilities of other proportions without correction for the effects of boundary-layer growth.

Effect of slot depth.- The center-line pressure distribution at $p_c/P_0 \approx 0.38$ ($M \approx 1.27$) is shown for constant-width slots of 1/8-, 1/2-, and 1-inch depth in figure 8. For the 1/8- and 1/2-inch-deep slots, the data of figure 3(a) were used directly; for the 1-inch slots, however, it was necessary to present data obtained by extrapolating the experimental pressures to lower values of p_c/P_0 . The pressure gradient in the initial expansion was independent of slot depth and for slots of 1/8- and 1/2-inch depth the extent of the initial expansion was nearly constant; with the deeper 1-inch slots, however, the initial expansion was carried to subchamber pressures. Differences in pressure ahead of the slots are probably associated with fairing of the nozzle blocks and are neglected in this discussion. The two characteristics nets from which the direction of flow and the mean pressure along the wall were obtained are presented for the half-nozzle. Convergence of the expansion lines on a point very close to the slot origin is indicative of an approach to the Prandtl-Meyer turn characteristic of the expansion from the end of a free jet or at the throat of a minimum-length nozzle. The flow angle along the wall, plotted as θ_w against x/h , increased abruptly at the upstream end of the slotted region and decreased thereafter to zero at $x/h \approx 3/4$. Maximum turning experienced with the deepest slots approached two-thirds of the calculated free-jet expansion; reducing slot depth from 1 inch to 1/2 or 1/8 inch reduced the initial turning by approximately 25 percent. The angle of flow along the slot downstream of the initial expansion was also reduced by the decrease in slot depth, and with the 1/8-inch depth, the direction of flow through the slots was reversed (air flowing into the channel) at $x/h = 0.66$. At this Mach number, $M \approx 1.27$, the pressure variation along the reflection plane was least with 1/2-inch-deep slots; at higher Mach numbers, reducing the slot depth to 1/8 inch resulted in more uniform flow.

Effect of slot width and free area ratio.- The effect of simultaneous variation of slot width and of the free area ratio of the slotted boundary is shown in figure 3(b). These curves were taken from cross plots of data

obtained in the $2\frac{1}{4}$ -by- $4\frac{1}{2}$ -inch channel with reflection plane (effective height, 9 inches). The slot widths investigated were 0.029-, 0.057-, and 0.100-inch, slot depth was constant at $1/2$ inch and spacing constant at $1/4$ inch; the corresponding free area ratios of the slotted boundaries were $1/9$, $1/5$, and $1/3$. At a chamber pressure ratio of 0.440, almost identical results were obtained with the 0.057- and 0.100-inch slots; however, reducing slot width to 0.029 inch (free area ratio, $1/9$) resulted in a substantial reduction in Mach number over the half tunnel height following the initial expansion. Agreement of the axial pressure distributions with $1/3$ - and $1/5$ -open boundaries at $p_c/P_o = 0.440$ can occur only if air is drawn across the slotted boundary into the chamber at identical rates of flow. If the slots are regarded as thick plate orifices, it follows that the discharge coefficient for the 0.057-inch slots is greater than that of the 0.100-inch slots by the ratio of the difference in free area ratio of the walls. Similarly, the lower Mach number obtained between $x/h = 0.25$ to 0.75, using 0.029-inch slots indicates that the discharge coefficient of these slots is not greater than that of the wider 0.057- or 0.100-inch openings by the ratio of free area ratios.

By reducing the chamber pressure ratio, the rate of air flow across the slotted boundary is increased and higher Mach numbers are generated until choking occurs. At p_c/P_o of 0.375 and 0.340, the axial pressure curves for the various wall configurations are well-separated. The general equality of the solid curves at pressure ratios of 0.375 and 0.340 indicates that with the $1/9$ -open boundary the 0.029-inch slots are choked at $p_c/P_o \cong 0.375$. With this configuration, channel lengths in excess of the height are necessary to generate Mach numbers greater than 1.2 ($\frac{p}{P_o} = 0.412$). Although the $1/5$ -open (0.057 inch) slots are not choked within the range of this investigation, it is apparent from the increased spread between the pressure in the chamber and the local pressure at the end of the initial expansion that these slots are approaching the choked conditions at $p_c/P_o = 0.340$. With the $1/3$ -open boundary, the initial expansion is carried to pressures substantially below the chamber pressure; slot choking therefore is not imminent.

A more detailed picture of the effect of increasing slot width and free area ratio is obtained by comparison of figures 9(a) and (b). Data for these figures were taken from center-line surveys carried out to $x/h \approx 2.6$ in the $6\frac{1}{4}$ -by- $4\frac{1}{2}$ -inch channel with slots in both $6\frac{1}{4}$ -inch walls, figures 5(a) and (b). As in tests using the reflection plane (fig. 8), the initial expansion occurs as an abrupt turn for both wall configurations. At Mach numbers on the order of 1.1, the flow angle

relative to the wall was essentially unaffected by changing slot width between 0.037 and 0.066. As in earlier tests in this range of slot sizes and chamber pressure ratios, the slot discharge coefficient increases as the slots become smaller. At higher Mach numbers choking in the slots appears to limit the rate of flow through the less open boundary; this limitation of the initial expansion appears advantageous in the $4\frac{1}{2}$ -by- $6\frac{1}{4}$ -inch channel, however, since at $x/h > 1$ the pressure variation along the tunnel and the variations in flow angle along the wall decrease with decreasing slot width and free area.

Effect of slot width and slot separation.- In the previously discussed configurations in which slot width was variable, the free area ratio of the boundary was also variable since the separation of the slots was constant. The effect of simultaneous changes in slot width and separation at constant free area ratio is shown by comparison of the center-line pressure distributions of figures 5(b) and (c). To facilitate comparison of these data, interpolated curves from figure 5(b) have been superimposed on the experimental distributions of figure 5(c) at corresponding values of the chamber pressure ratio. As previously discussed, the initial rate of expansion was essentially unchanged when slot width and spacing were simultaneously increased by a factor of 18. Immediately downstream of the initial expansion, however, the Mach numbers obtained with the larger slots at chamber pressures corresponding to Mach numbers on the order of 1.15 or greater, were appreciably smaller than those obtained with the closer spacing of small slots. Thus increasing slot width and spacing has in this Mach number range decreased the flow rate per unit area. It will be noted that this comparison is somewhat extreme in that the separation of the small slots is of the order of 6 percent of the tunnel height and that of the large slots is 110 percent of the tunnel height. In determining separation of the wide slots, the tunnel side wall is considered as the midpoint between adjacent slots. The center-line surveys are accordingly in a vertical plane through the slot center line; static-pressure surveys in other vertical planes indicate substantial differences as a result of three-dimensional effects not present in configurations utilizing closely spaced slots.

A similar comparison at slightly higher Mach numbers in the $2\frac{1}{4}$ -by- $4\frac{1}{2}$ -inch channel with the reflection-plane (effective height, 9 inches) setup fails to show any substantial difference between initial expansion with variation of slot separation. This is shown in figure 3(a) where interpolated curves from the $1/2$ -inch-deep single-slot configuration of reference 1 are superimposed on the curves from tests of slots of $1/2$ -inch depth at the same chamber pressure ratios. In this comparison, data from tests of 0.057-inch slots at 0.25-inch separation are compared with 0.40-inch slots at 1.85-inch separation

in a channel whose effective height was 9 inches; in terms of channel height the corresponding separation was 3 and 20 percent, respectively, whereas in the $4\frac{1}{2}$ -by- $6\frac{1}{4}$ -inch channel the corresponding values were 6 and 110 percent.

Effect of taper in slot width.- Data obtained in tests of several wall configurations in which slot width was increased along straight tapers, presented in figures 5(d) to (h), are analyzed in figures 9(c) to 9(g). With a 1.25° taper opening into 0.037-inch slots in the $6\frac{1}{4}$ -by- $4\frac{1}{2}$ -inch channel, the center-line pressure distribution was appreciably less uniform, figures 9(a) and (c). Comparison of the characteristics diagrams and the flow-angle distribution along the wall shows that the introduction of the tapered entry to the slots reduced the rate of turning at the upstream end of the slots and reduced the total volume of air removed from the forward part of the tunnel (note reduction in area under the curve of θ_w against x/h). Similar results were obtained when 1.25° taper was used with the $1/5$ -open walls $w_s = 0.066$, figures 9(b) and (d). Comparison of the θ_w curves of figures 9(d) and 9(e) with figure 9(b) shows that the introduction of taper into the slot plan form to effect a more gradual opening of the boundary resulted in substantial reductions in the initial rate of expansion but for the $1/5$ -open boundary with 0.066-inch slots the resultant flow was not significantly improved. The maximum flow angles relative to the wall were obtained with 2.75° taper.

With the 1.25° tapered slots of configurations reported in figures 5(d) and (e) and figures 9(c) and (d), the separation of the individual slots at their maximum width was constant, 0.25 inch, the increase in slot width from 0.037 to 0.066 inch was therefore accompanied by an increase in the free area of the boundary and a reduction in the number of slots and an increase in tapered length. Comparison of the corresponding curves of figure 2 shows that the rate of opening of these slotted walls is approximately the same for the first $1\frac{3}{4}$ inches; in this region, however, the characteristics nets and the curves of θ_w against x/h of figures 9(c) and (d) indicates that the initial rate of turning in this region was greater for the narrower slots. The higher flow through the narrower slots is consistent with an earlier observation that decreasing slot width increases the flow coefficient of the slot. A similar comparison between data obtained in tests of slots of 0.066- and 0.143-inch width with 2.75° taper at the forward end, figures 9(e) and (f), also shows a higher rate of air flow across the upstream section of the narrow slots at Mach numbers close to unity with equal or greater flow across the wider slots, more open boundaries, at Mach numbers on the order of 1.2 or greater. Comparison of the rate of flow across the various boundary configurations beyond the point of the initial expansion is somewhat meaningless unless the slots have

become choked because the variations in angle downstream of the initial expansion are to a large extent determined by the characteristics of the initial expansion.

Although the taper angles used in these configurations were in general of the same order as those used to advantage in other installations, the length of taper relative to the tunnel height was much smaller as a result of the use of narrow, closely spaced slots. The generally unsatisfactory results obtained with these configurations suggests that taper length rather than taper angle is the significant parameter. This conclusion is further borne out by comparison of the data presented in figures 5(f) and (h) and figures 9(e) and (g) where results are presented of tests of 1/5-open boundaries differing in slot width from 0.066 to 0.225 inch and in taper length from approximately 0.3 to 1.05 channel heights. The initial expansion with the longer taper, wider slots, occurred at a somewhat slower rate than in previously discussed configurations; the amount of turning also was less than that observed with other tapered configurations opening into slots with approximately equal total free area. Compare the curves of θ_w against x/h in figure 9(g) with those in figures 9(d) and 9(e) in which the tapered sections were of the order of 0.7 and 0.3 tunnel height, respectively. Although the overexpansions with subsequent nonuniform flows have not been eliminated in this configuration with wide (0.225-inch) slots, an improvement, especially noticeable at Mach numbers of the order of 1.1 or less, has been effected, reemphasizing the desirability of long taper in slots designed for tunnels to operate at low supersonic Mach numbers.

Comparison of figures 5(e) with 5(g) and figures 9(d) with 9(f) shows the effect of increasing slot width and free area ratio at constant taper length (3 inches) and spacing (0.25 inch). At low Mach numbers ($M \leq 1.2$) the pressure variations along the axis of the channel were appreciably reduced by increasing slot width with the initial expansion effected at a slightly higher rate. At Mach numbers of the order of 1.3 or greater, the extent of the overexpansion increased with slot width and the resultant pressure variations along the axis were increased.

Effect of taper in slot depth.- The data of figures 6(a) and (b) and figures 10(a) and (b) were obtained in the $4\frac{1}{2}$ -by- $4\frac{1}{2}$ -inch tunnel with slots of identical plan form; the data of figure 6(a) were obtained with slots of constant depth (1/2 inch) while those of figure 6(b) were obtained with slots whose depth decreased linearly throughout the tapered region from 1/2 inch at the front of the slot to 1/16 inch at $x/h = 0.66$, the end of the plan-form taper. Comparison of typical center-line pressure distributions from these tests shows little change

in initial expansion rate, but indicates a marked reduction in the magnitude of the overexpansion and subsequent recompression with slots tapered in depth as well as in width. Comparison of the curve of θ_w against x/h for these two slot configurations shows that this improvement, effected by introducing a variation in the depth along the slot, stems largely from the reduction in the maximum flow angularity reached in the initial expansion establishing equilibrium between the chamber and the channel with smaller variations in flow direction along the slotted boundary. With these slots, tapered in both width and depth, the mean pressure along the channel boundary approaches the chamber pressure very closely at the downstream end of the survey; it therefore appears probable that uniform flow may be obtained over any desired length of test section by simply extending the channel to the desired point.

CONCLUSIONS

From the results of this investigation of the transonic flow in rectangular tunnels with slotted top and bottom boundaries, it is concluded that:

1. Increasing tunnel height-width ratio reduces the amount of expansion which can be obtained in a given distance from the slot entrance with slots of equal air-flow capacity.
2. In tunnels whose width is approximately equal to the height, Mach number variations of 0.01 or less can be achieved up to a Mach number of at least 1.4 by the use of slots whose width increases and whose depth decreases from the beginning of the slot for a distance equal to $2/3$ of the tunnel height.
3. At high Mach numbers choking of the slots in boundaries of low free area ratio necessitates very long slotted sections.
4. A tapered entry to constant-depth slots reduces the initial rate of expansion but may cause increased overexpansion with a resulting increase in pressure disturbances along the tunnel.

Langley Aeronautical Laboratory,
National Advisory Committee for Aeronautics,
Langley Field, Va.

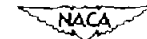
REFERENCES

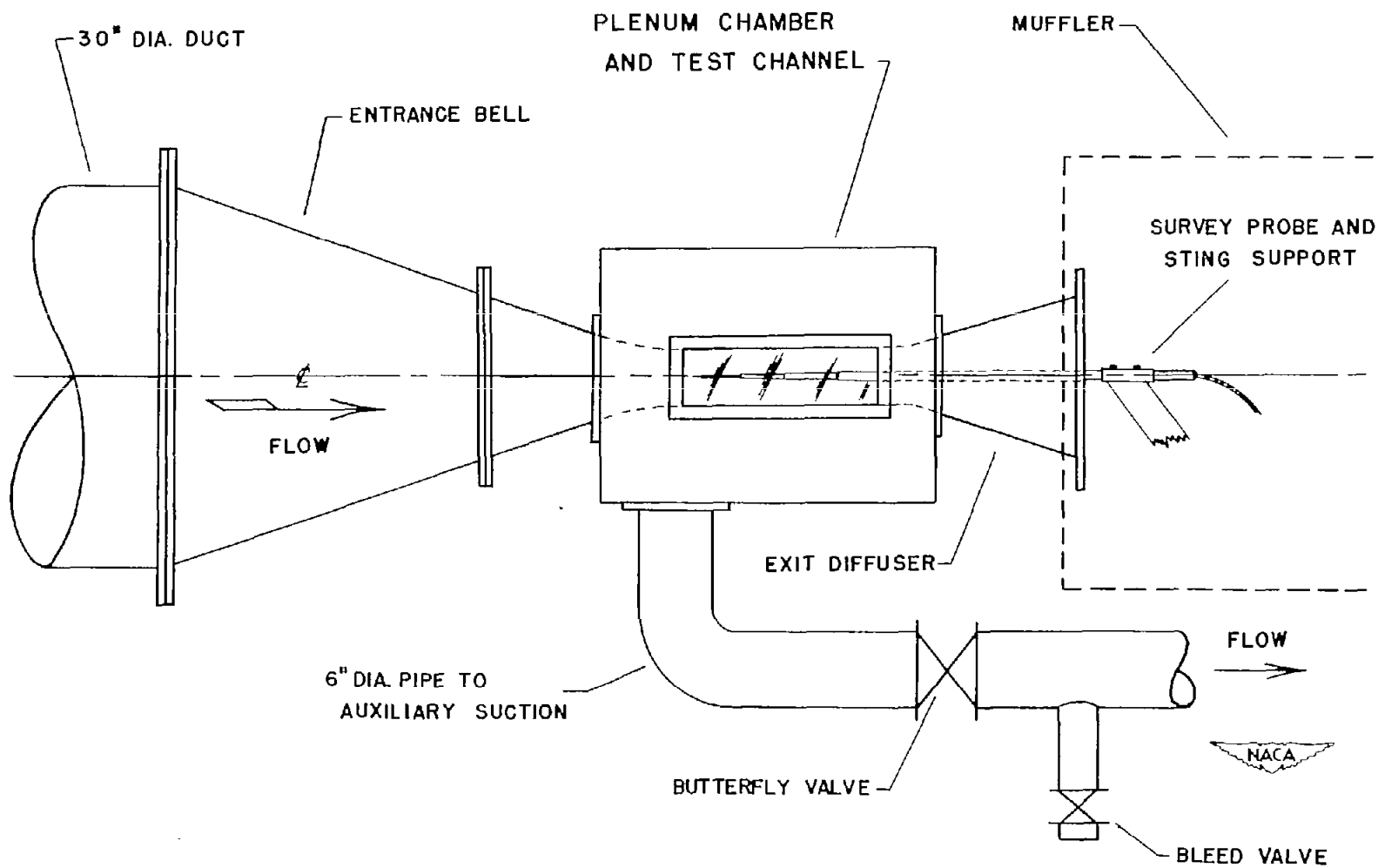
1. Nelson, William J., and Bloetscher, Frederick: Preliminary Investigation of a Variable Mach Number Two-Dimensional Supersonic Tunnel of Fixed Geometry. NACA RM L9D29a, 1949.
2. Osborne, James I., and Zeck, Howard: Progress Report on Development of a Transonic Test Section for the Boeing Wind Tunnel (BWT 188). Vol. I - December 1950 to June 1951. Doc. No. D-11955, Boeing Airplane Company, Sept. 1951.
3. Goethert, Bernhard H.: Investigations on Transonic Test Sections at the Wind Tunnel Branch, AMC-Wright Field. Air Materiel Command, Wright Field, Sept. 25, 1950.
4. Ward, Vernon G., Whitcomb, Charles F., and Pearson, Merwin O.: An NACA Transonic Test Section With Tapered Slots Tested at Mach Numbers to 1.26. NACA RM L50B14, 1950.
5. Wright, Ray H., and Ritchie, Virgil S.: Characteristics of a Transonic Test Section With Various Slot Shapes in the Langley 8-Foot High-Speed Tunnel. NACA RM L51H10, 1951.

TABLE I.- DIMENSIONS OF CHANNELS AND SLOT CONFIGURATIONS

Channel size, in.	h, in.	h/w	nw_s/w	d_s , in.	w_s , in.	ϕ , deg	L, in.	n	Over-all length of slot, in.	Slot separation, in.	Figure
$2\frac{1}{4}$ by $4\frac{1}{2}$	9.0	4.00	$a_{1/5}$	1/8	0.057	180	0	7	12.0	0.25	3(a), 8
	9.0	4.00	$a_{1/5}$	1/2	.057	180	0	7	12.0	.25	3(a), 8
	9.0	4.00	$a_{1/5}$	1	.057	180	0	7	12.0	.25	3(a), 8
	9.0	4.00	$a_{1/9}$	1/2	.029	180	0	7	12.0	.25	3(b)
	9.0	4.00	$a_{1/3}$	1/2	.100	180	0	5	12.0	.25	3(b)
$6\frac{1}{4}$ by $4\frac{1}{2}$	9.0	1.44	1/5	1/2	.066	180	0	19	15.0	.25	4
	4.5	.72	1/5	1/2	.066	180	0	19	15.0	.25	5(b), 9(b)
	4.5	.72	$a_{1/5}$	1/2	1.200	180	0	1	15.0	5.00	5(c)
	4.5	.72	1/8	1/2	.037	180	0	21	15.0	.25	5(a), 9(a)
	4.5	.72	1/8	1/2	.037	1.25	1.68	21	13.7	.25	5(d), 9(c)
	4.5	.72	1/5	1/2	.066	1.25	3.00	19	15.0	.25	5(e), 9(d)
	4.5	.72	1/5	1/2	.066	2.75	1.38	19	13.4	.25	5(f), 9(e)
	4.5	.72	1/2.9	1/2	.143	2.75	2.98	15	15.0	.25	5(g), 9(f)
	4.5	.72	1/4.6	1/2	.225	2.75	4.72	6	15.0	.90	5(h), 9(g)
$4\frac{1}{2}$ by $4\frac{1}{2}$	4.5	1.00	1/8	1/2	.141	2.75	2.96	4	12.8	.90	6(a), 10(a)
	4.5	1.00	1/8	1/2 to 1/16	.141	2.75	2.96	4	12.8	.90	6(b), 10(b)

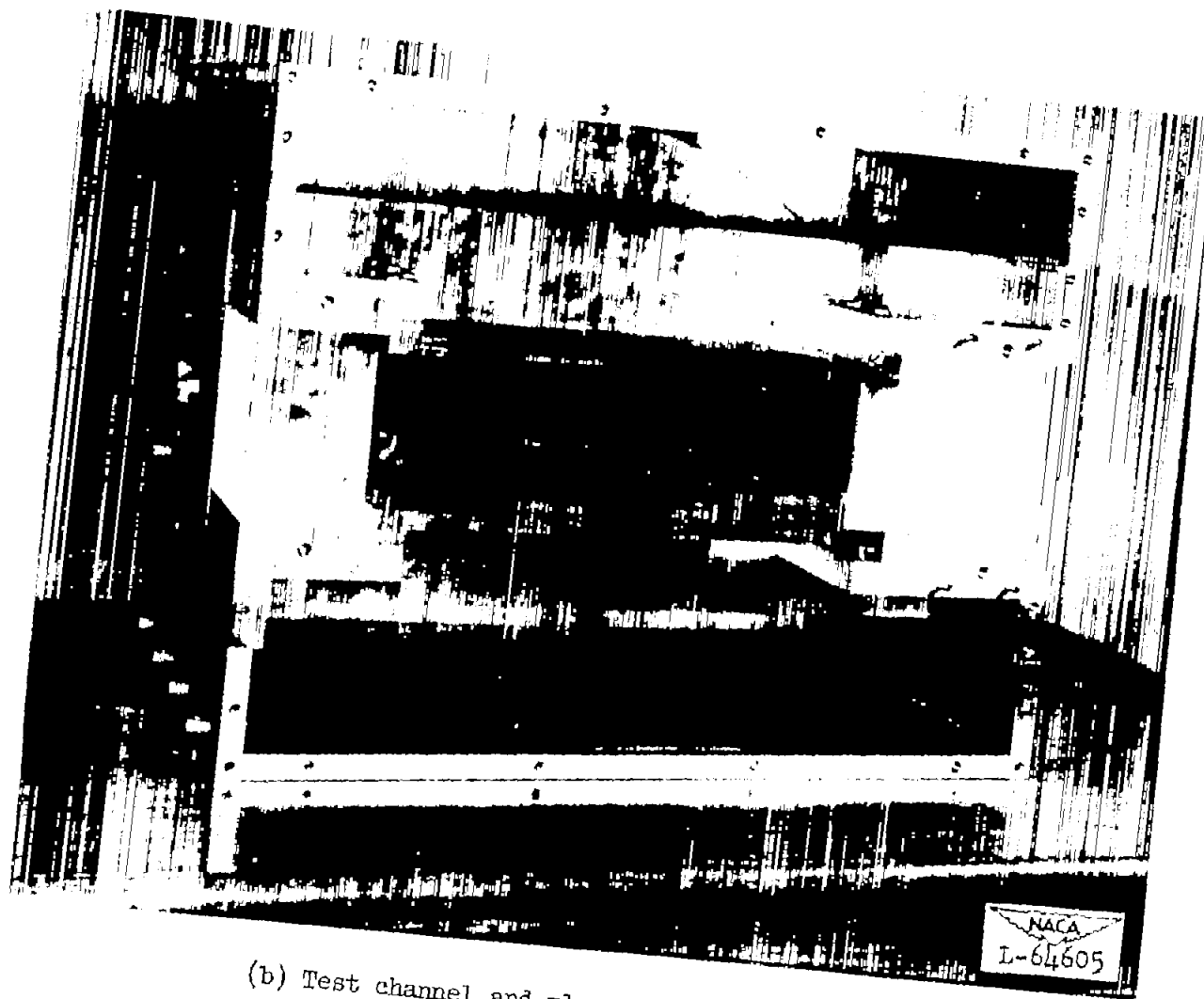
^aIncludes 0.025-inch gaps between side walls and slotted boundary.





(a) General arrangement.

Figure 1.- Test equipment.



(b) Test channel and plenum chamber assembly;

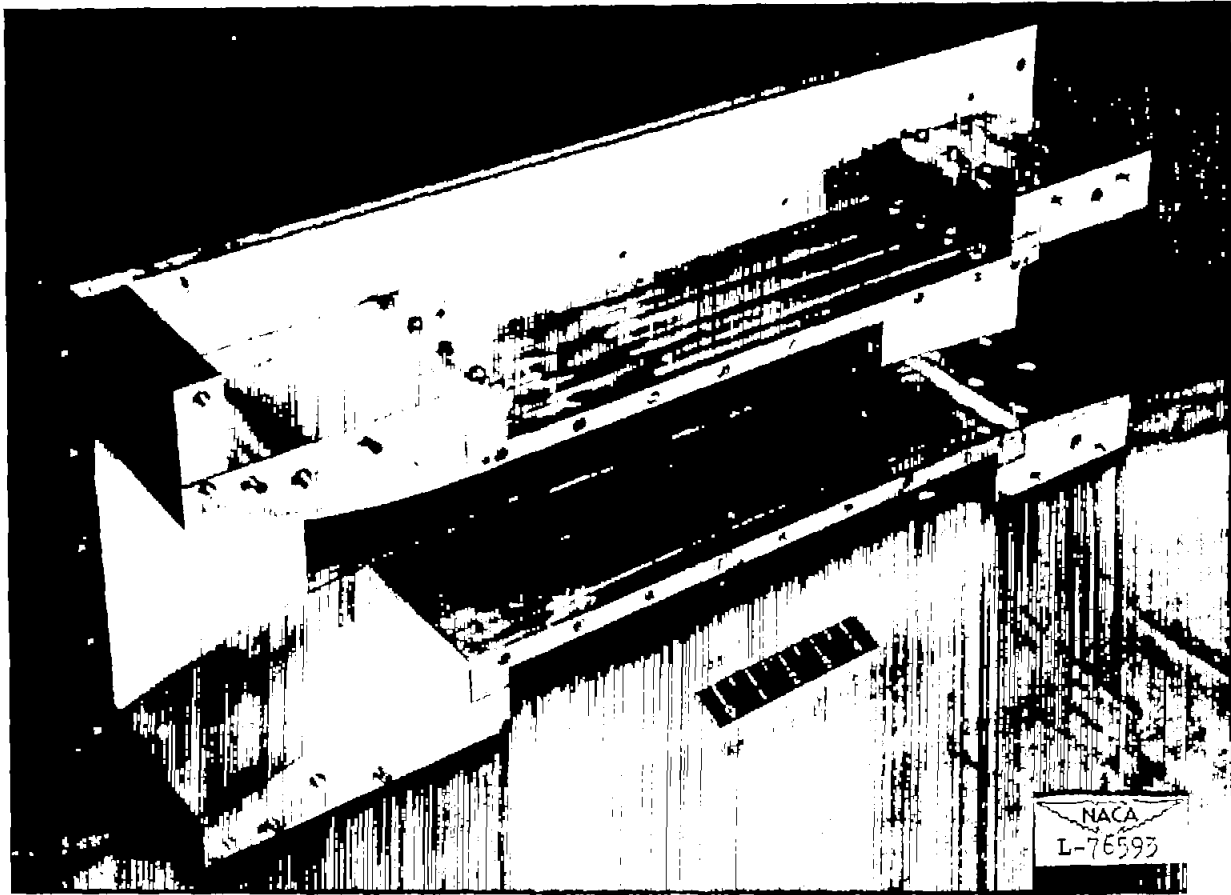
$$w = 6\frac{1}{4} \text{ inches; } h = 4\frac{1}{2} \text{ inches.}$$

Figure 1.- Continued.



(c) Test channel and slotted wall assembly; $w = 6\frac{1}{4}$ inches;
 $h = 4\frac{1}{2}$ inches; $nw_s/w = 1/5$; $w_s = 0.066$ inch; $n = 19$;
 $\Phi = 180^\circ$.

Figure 1.- Continued.



(d) Test channel and slotted wall assembly; $w = 4\frac{1}{2}$ inches;
 $h = 4\frac{1}{2}$ inches; $nw_s/w = 1/8$; $w_s = 0.141$ inch; $n = 4$;
 d_s , variable along taper; $\Phi = 2.75^\circ$.

Figure 1.- Concluded.

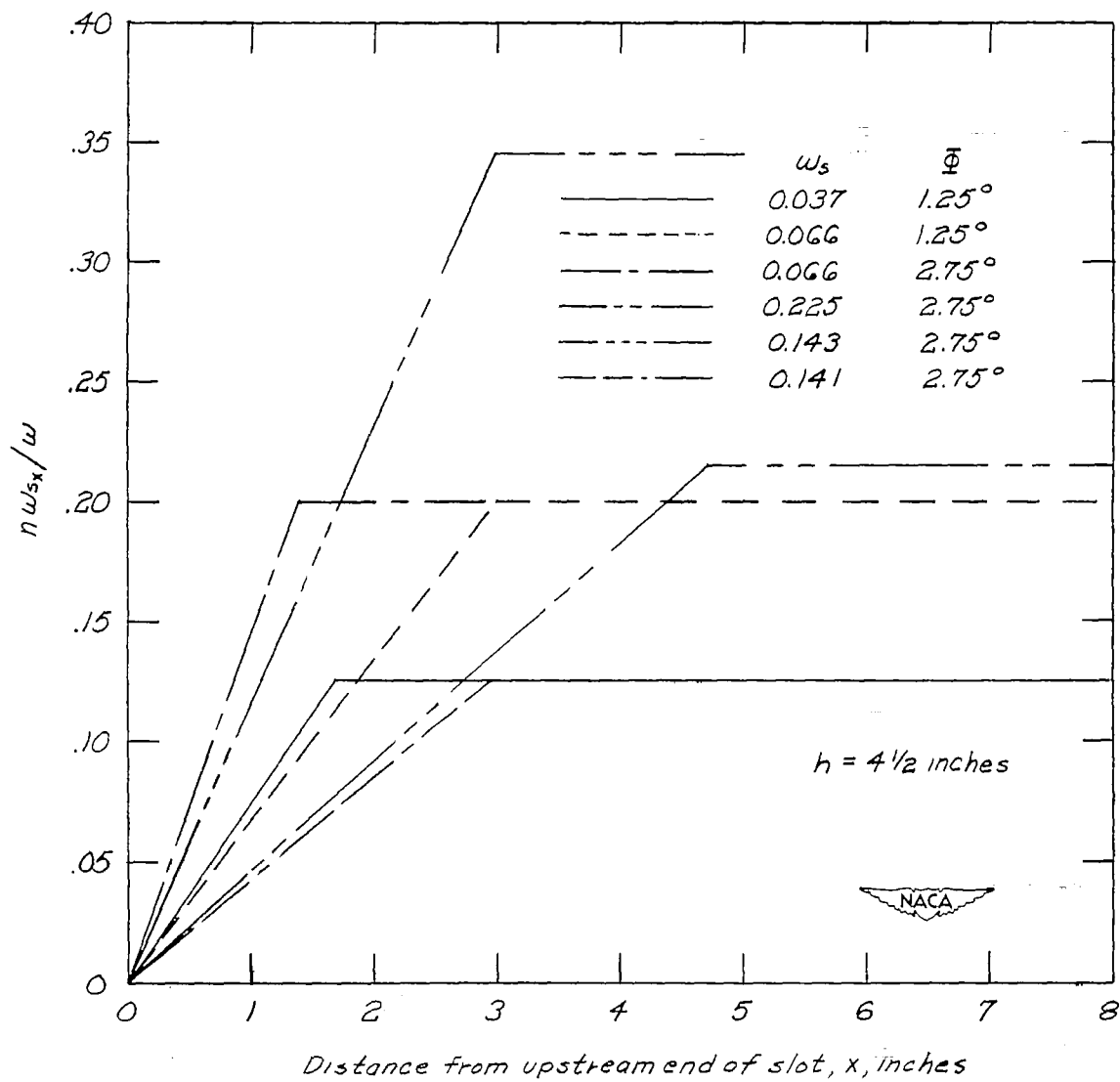
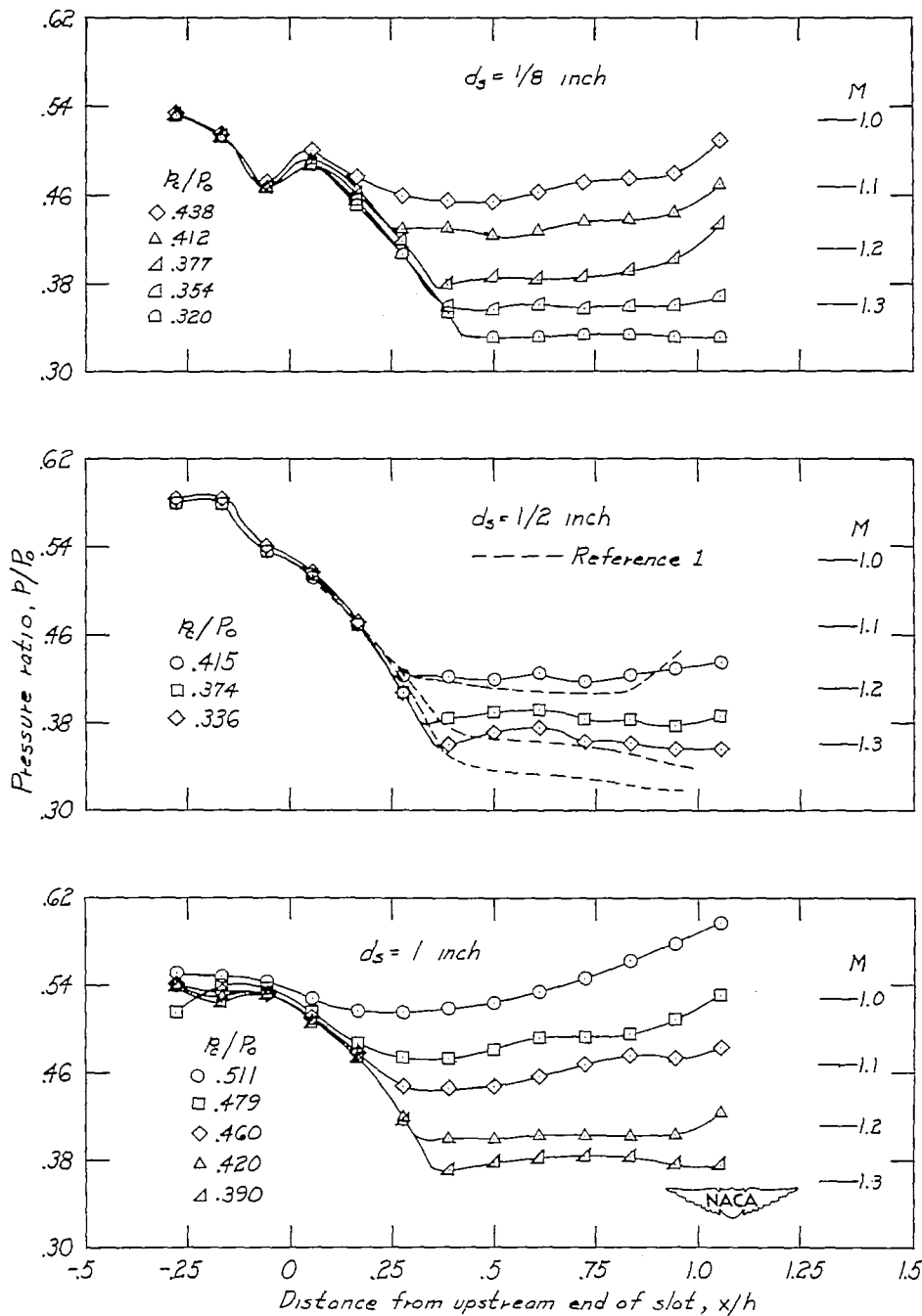
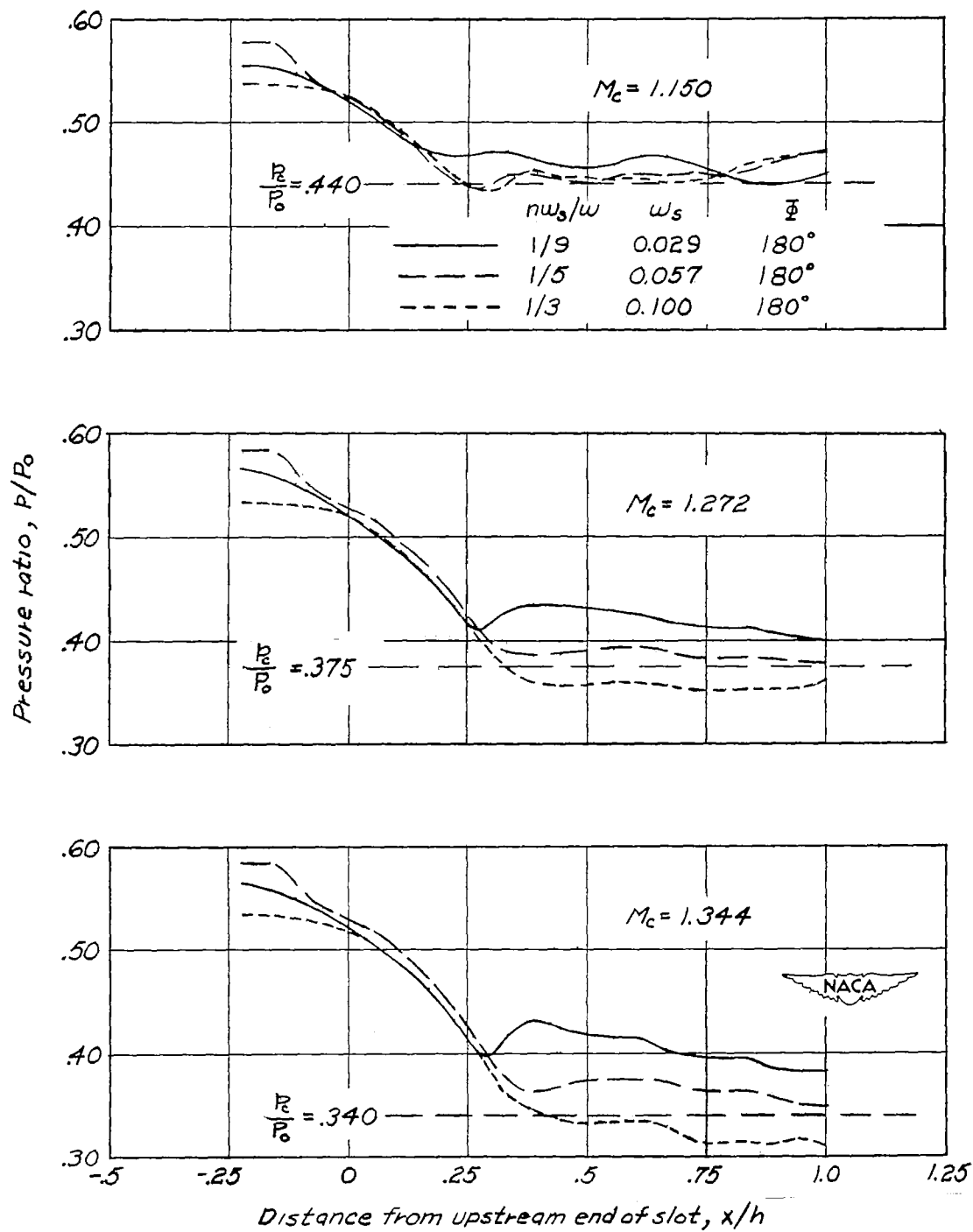


Figure 2.- Variation of free area ratio at any point with distance from upstream end of tapered slot.



(a) $nw_g/w = 1/5$; $w_g = 0.057$ inch; $n = 7$; $\phi = 180^\circ$.

Figure 3.- Pressure distribution along reflection plane; $w = 2\frac{1}{4}$ inches;
 $h = 9$ inches.



(b) $nw_s/w = 1/9, 1/5, 1/3$; $w_s = 0.029, 0.057, 0.100$ inch; $n = 7, 7, 5$; $\Phi = 180^\circ$.

Figure 3.- Concluded.

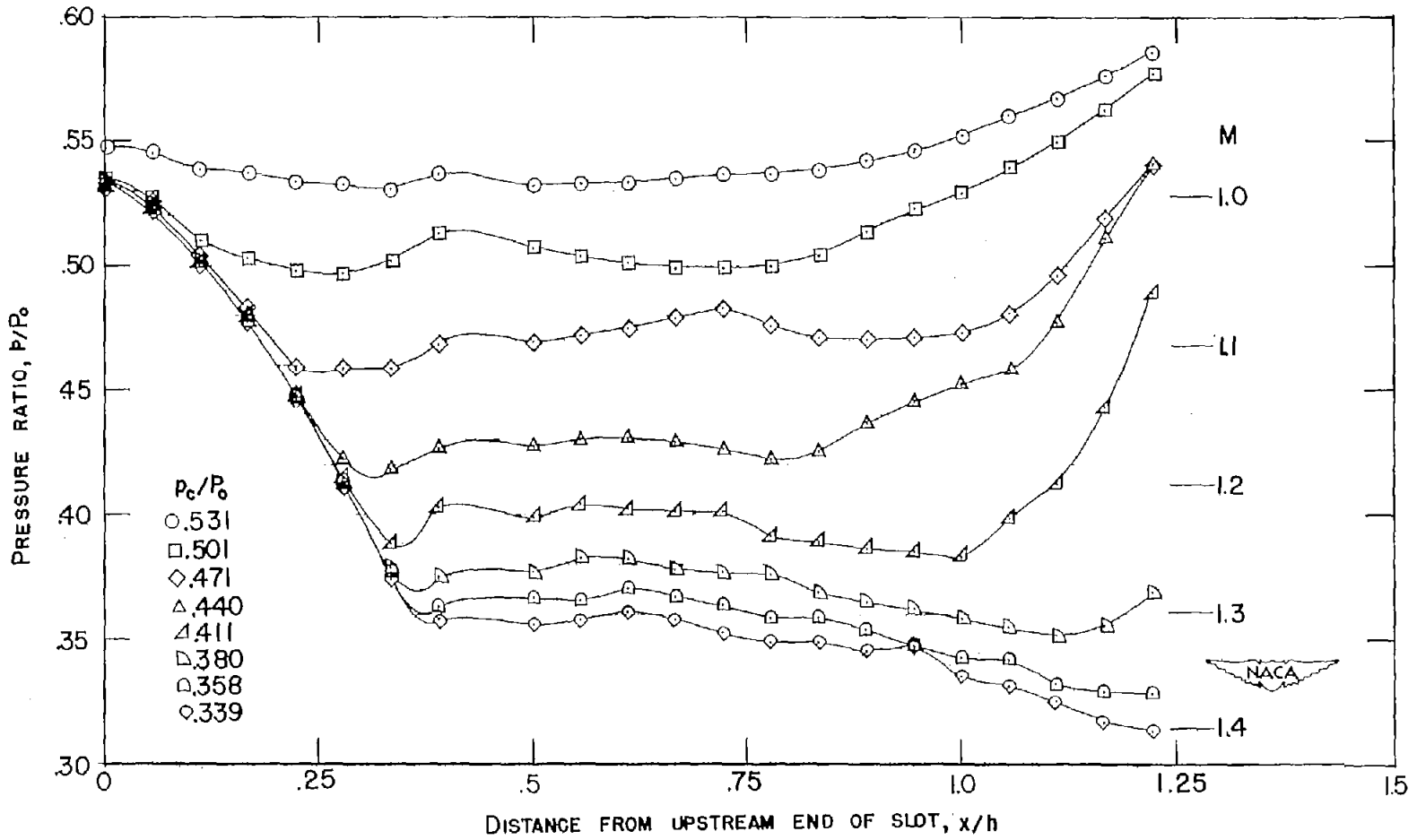
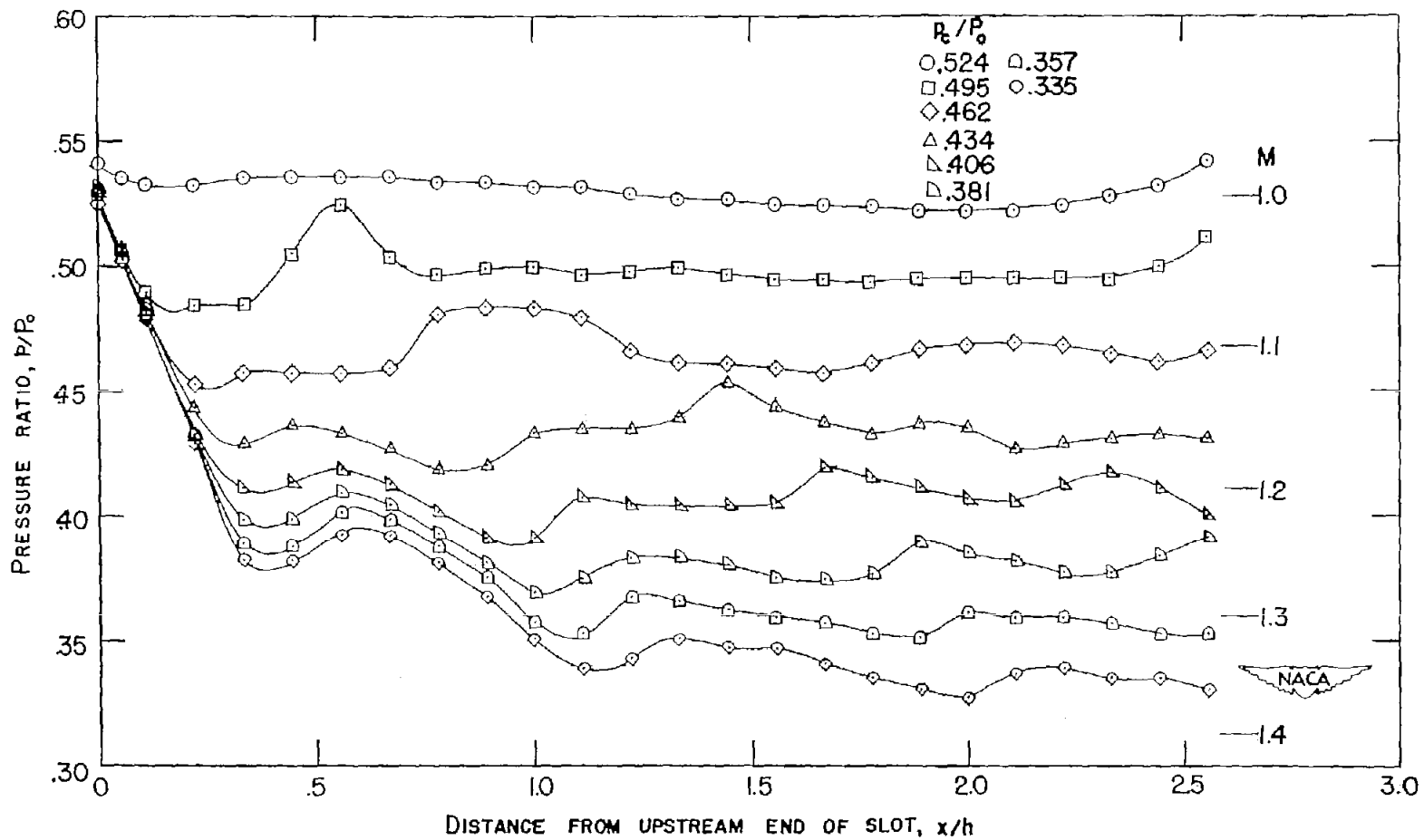
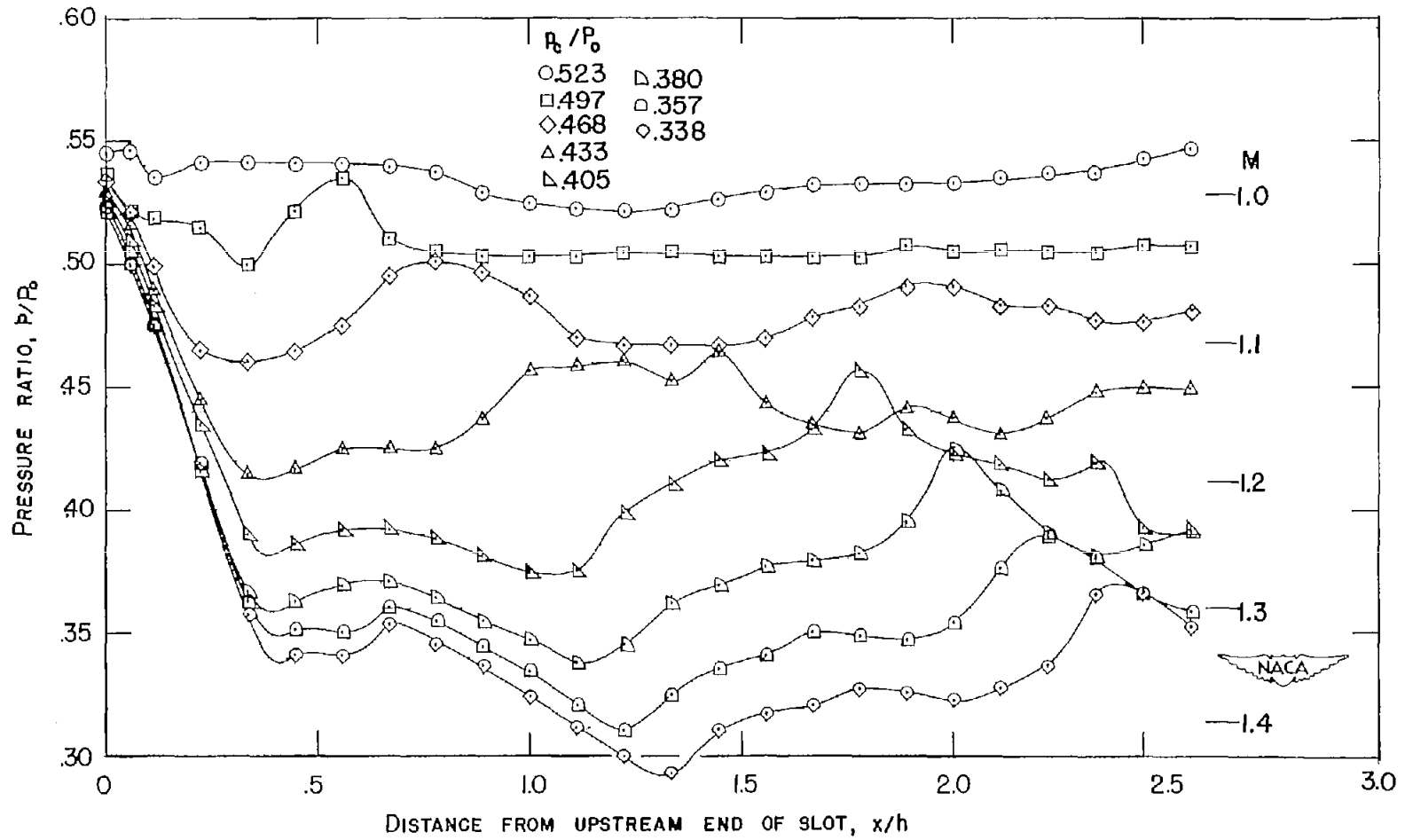


Figure 4.- Pressure distribution along reflection plane; $w = \frac{6}{4}$ inches;
 $h = 9$ inches; $nw_B/w = 1/5$; $w_B = 0.066$ inch; $n = 19$; $\phi = 180^\circ$.



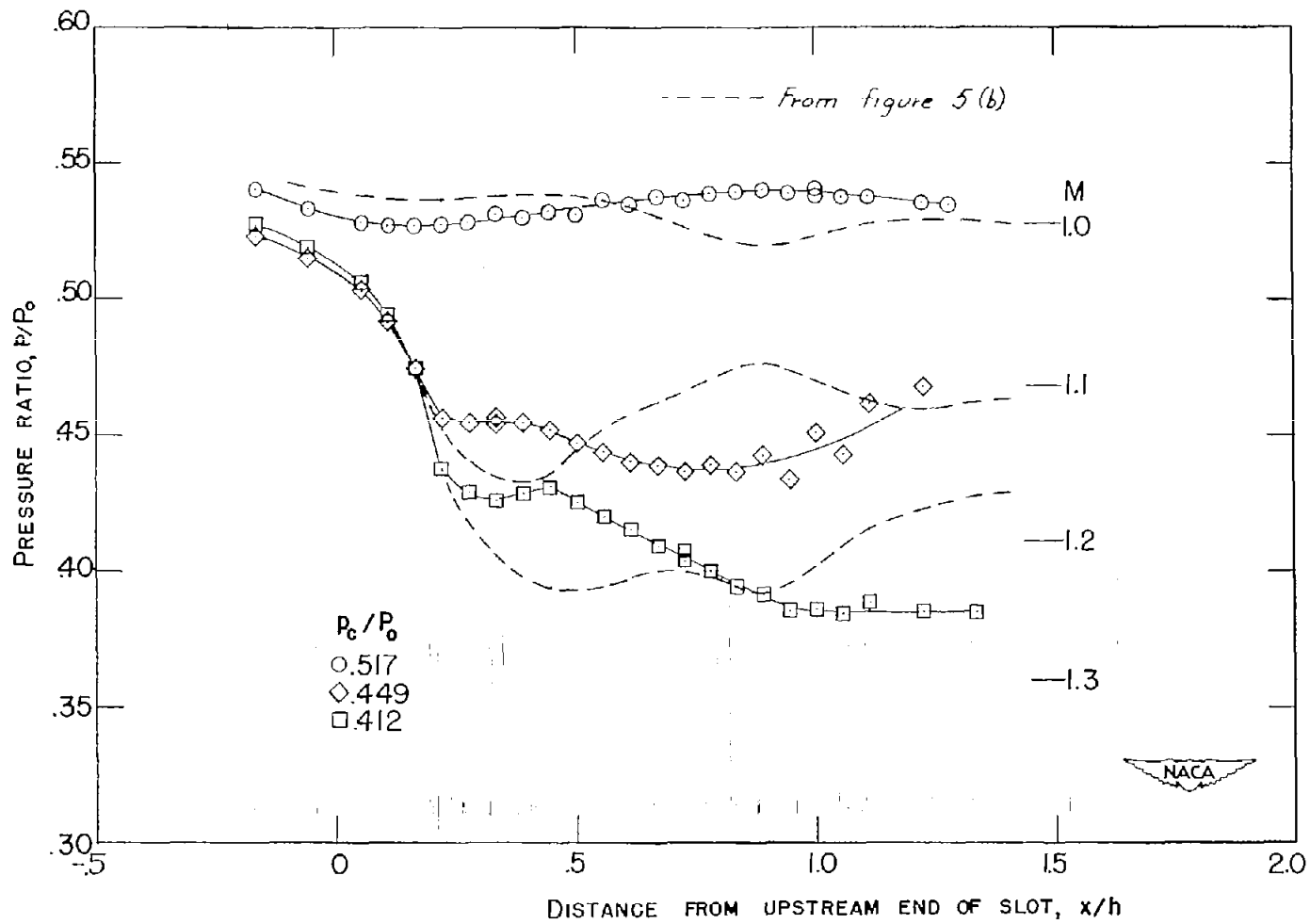
(a) $nw_s/w = 1/8$; $w_s = 0.037$ inch; $n = 21$; $\phi = 180^\circ$.

Figure 5.- Pressure distribution along center line; $w = 6\frac{1}{4}$ inches;
 $h = 4\frac{1}{2}$ inches.



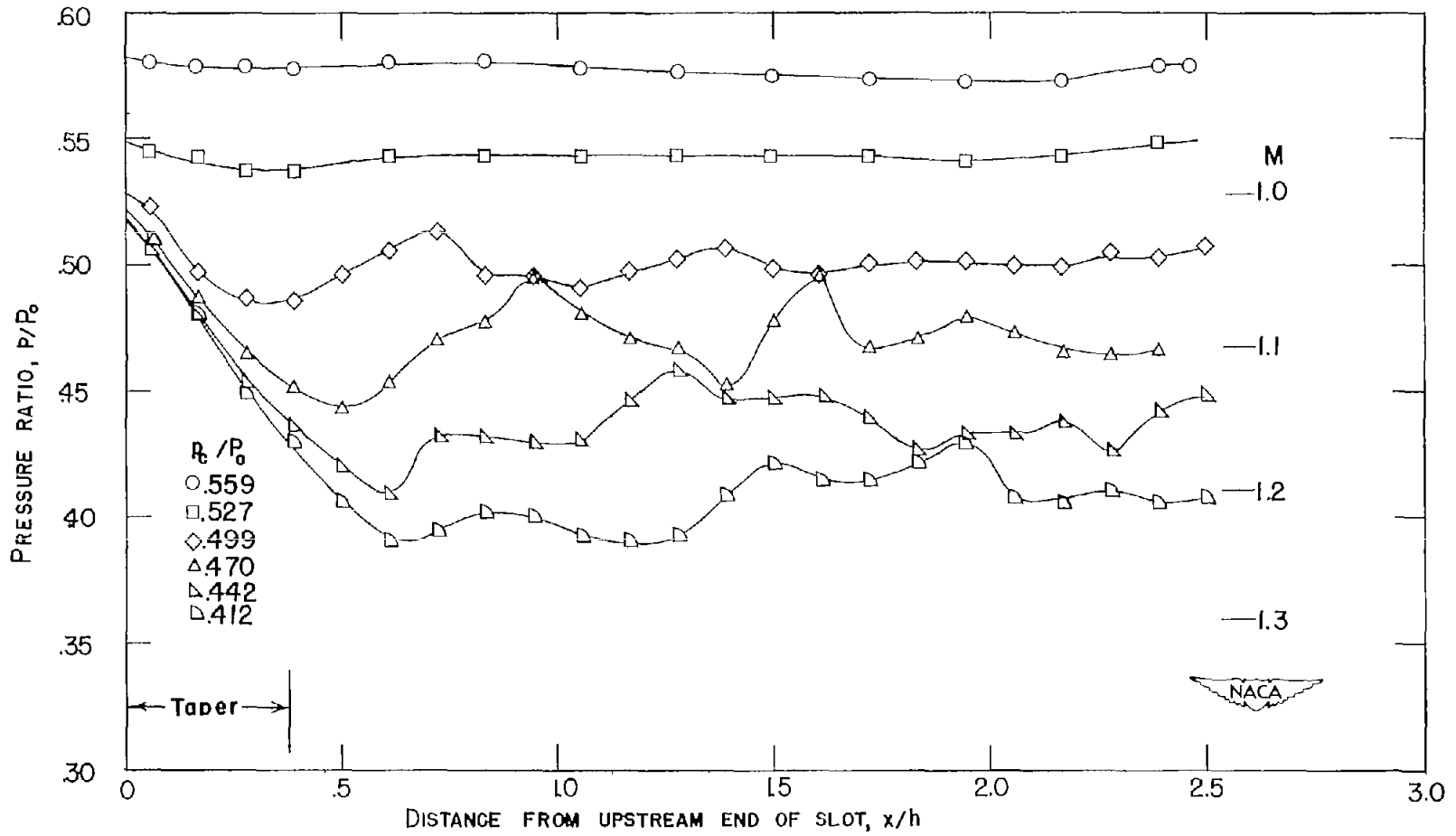
(b) $nw_s/w = 1/5$; $w_s = 0.066$ inch; $n = 19$; $\phi = 180^\circ$.

Figure 5.- Continued.



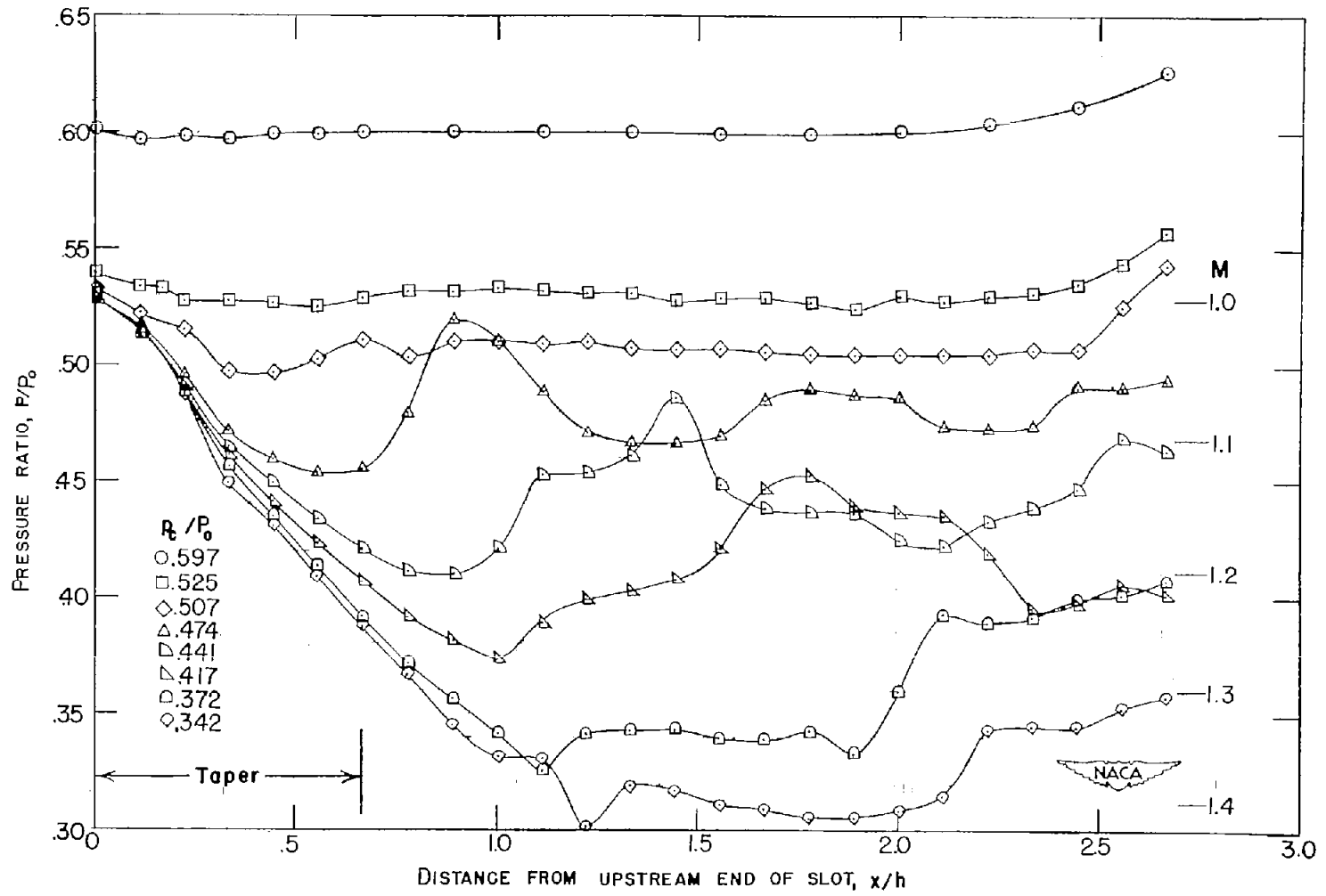
(c) $nw_g/w = 1/5$; $w_g = 1.20$ inches; $n = 1$; $\Phi = 180^\circ$.

Figure 5.- Continued.



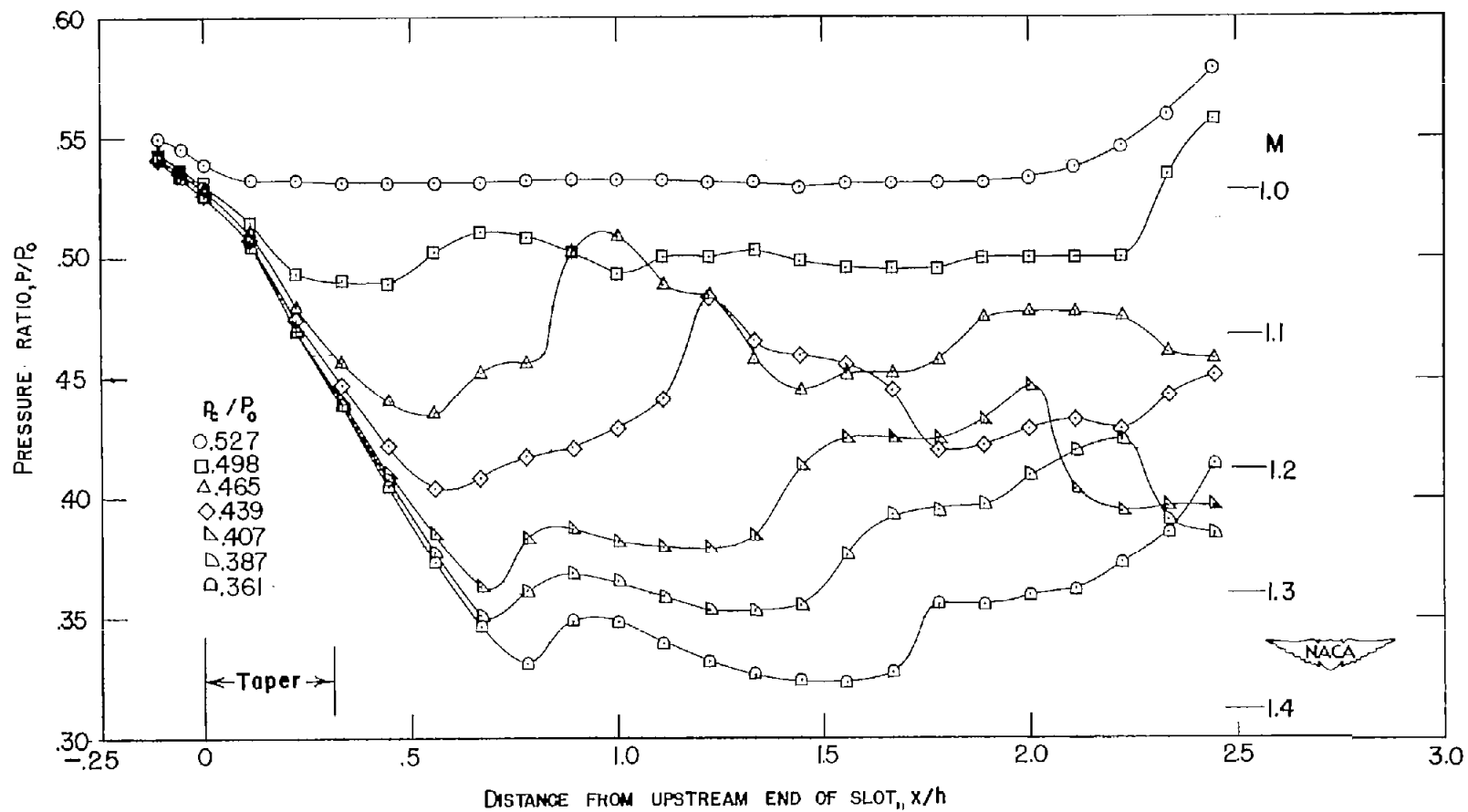
(d) $nw_B/w = 1/8$; $w_B = 0.037$ inch; $n = 21$; $\phi = 1.25^\circ$.

Figure 5.- Continued.



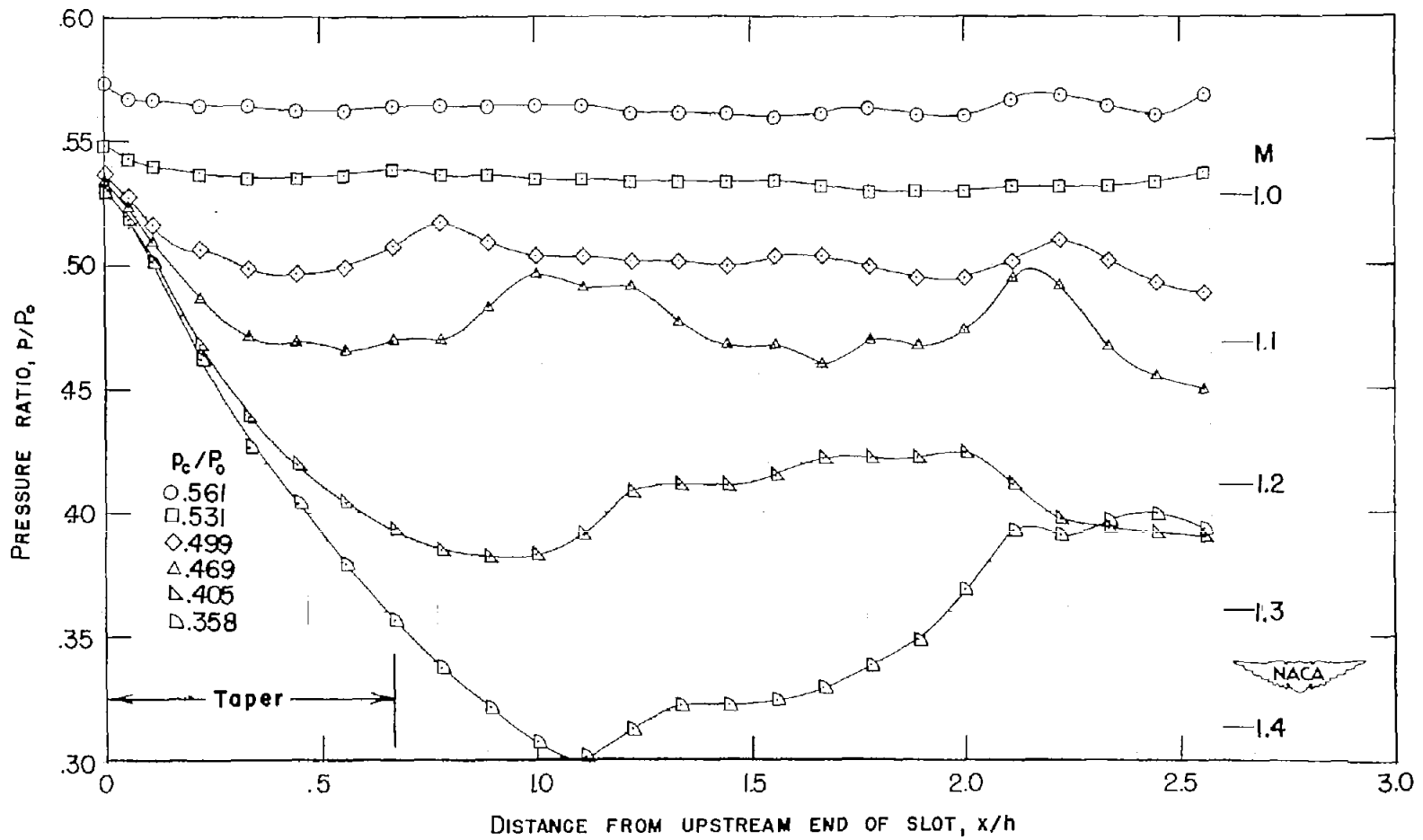
(e) $nw_s/w = 1/5$; $w_s = 0.066$ inch; $n = 19$; $\phi = 1.25^\circ$.

Figure 5.- Continued.



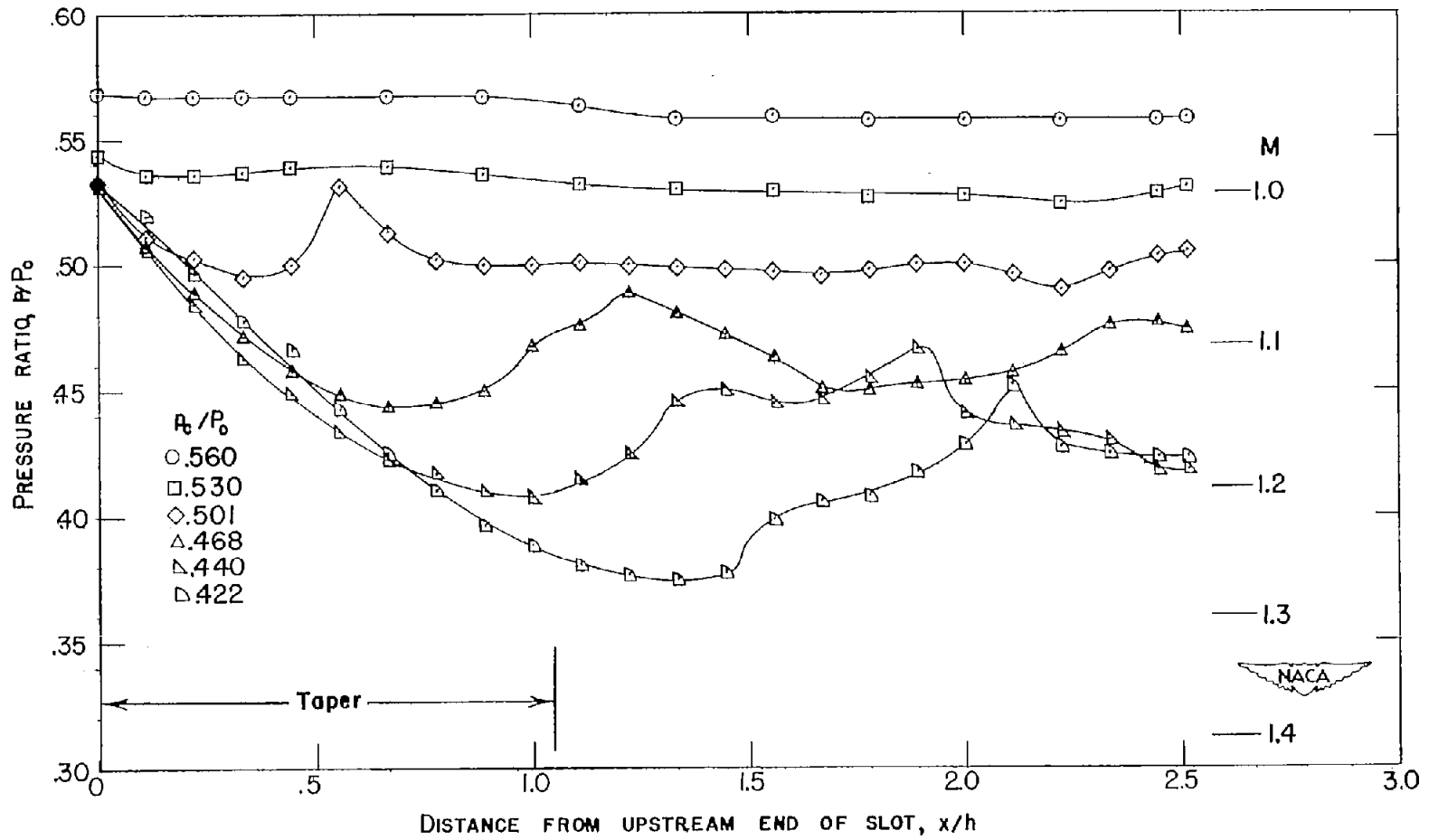
(f) $nw_g/w = 1/5$; $w_g = 0.066$ inch; $n = 19$; $\phi = 2.75^\circ$.

Figure 5.- Continued.



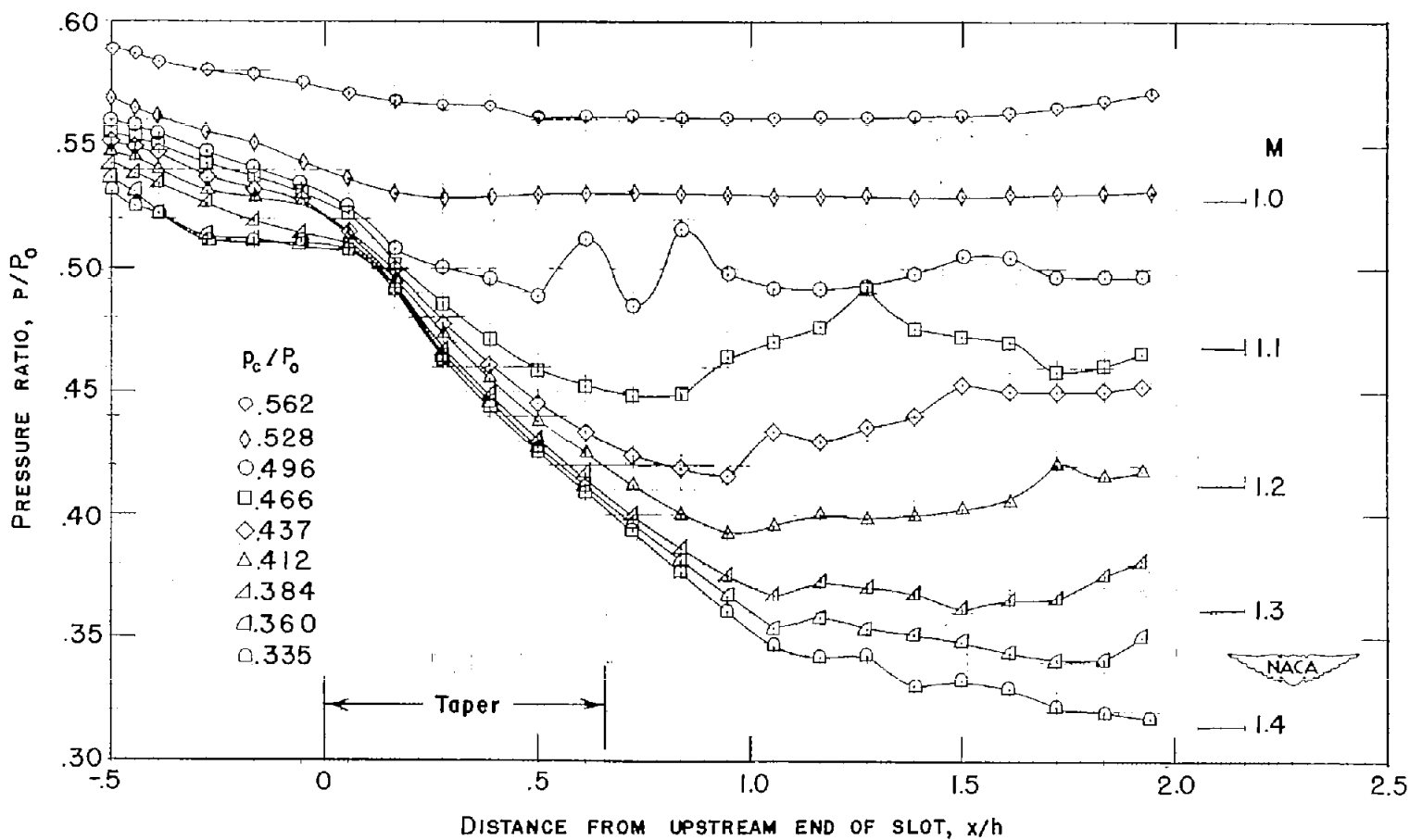
(g) $nw_S/w = 1/2.9$; $w_S = 0.143$ inch; $n = 15$; $\phi = 2.75^\circ$.

Figure 5.- Continued.



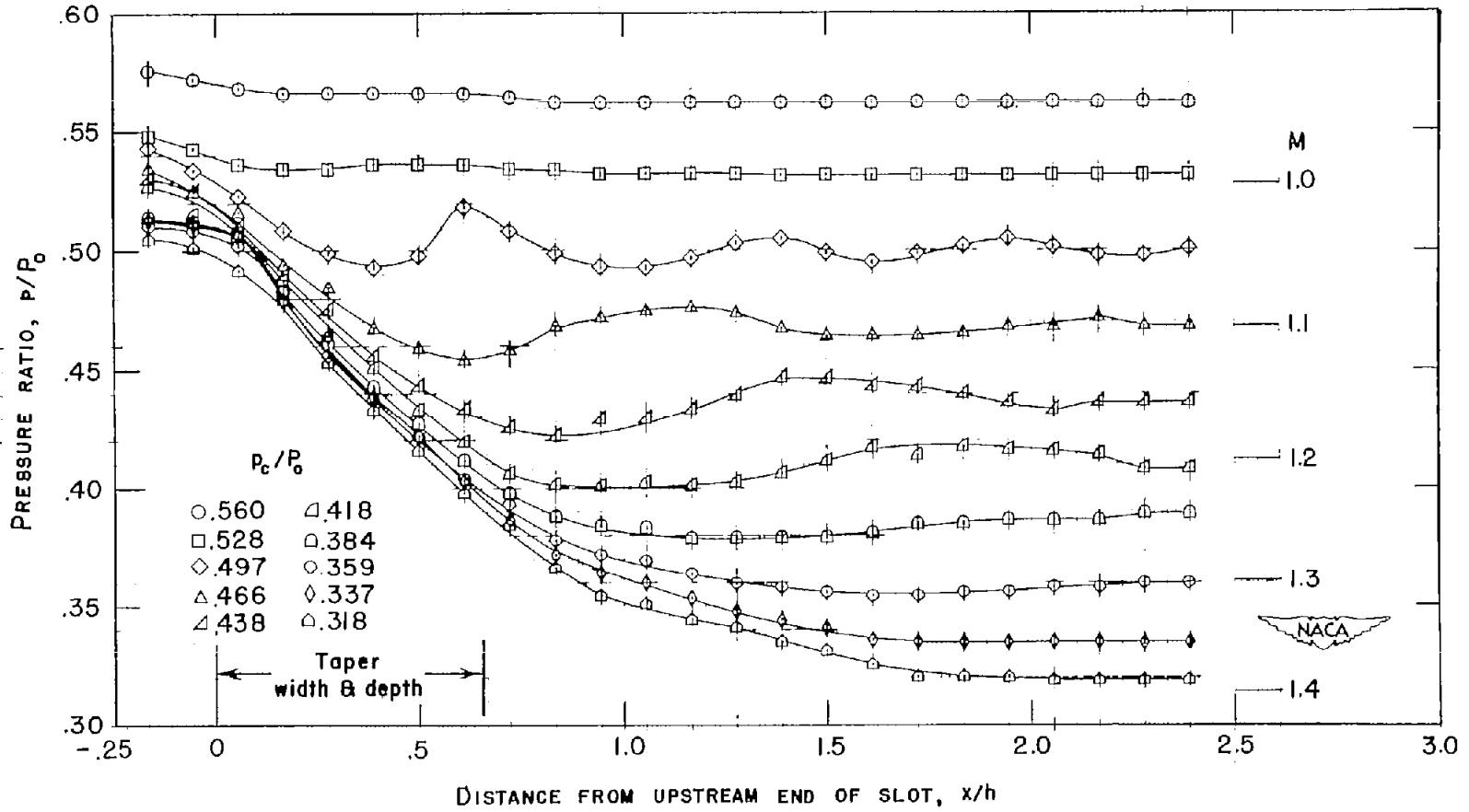
(h) $nw_B/w = 1/4.64$; $w_B = 0.225$ inch; $n = 6$; $\phi = 2.75^\circ$.

Figure 5.- Concluded.



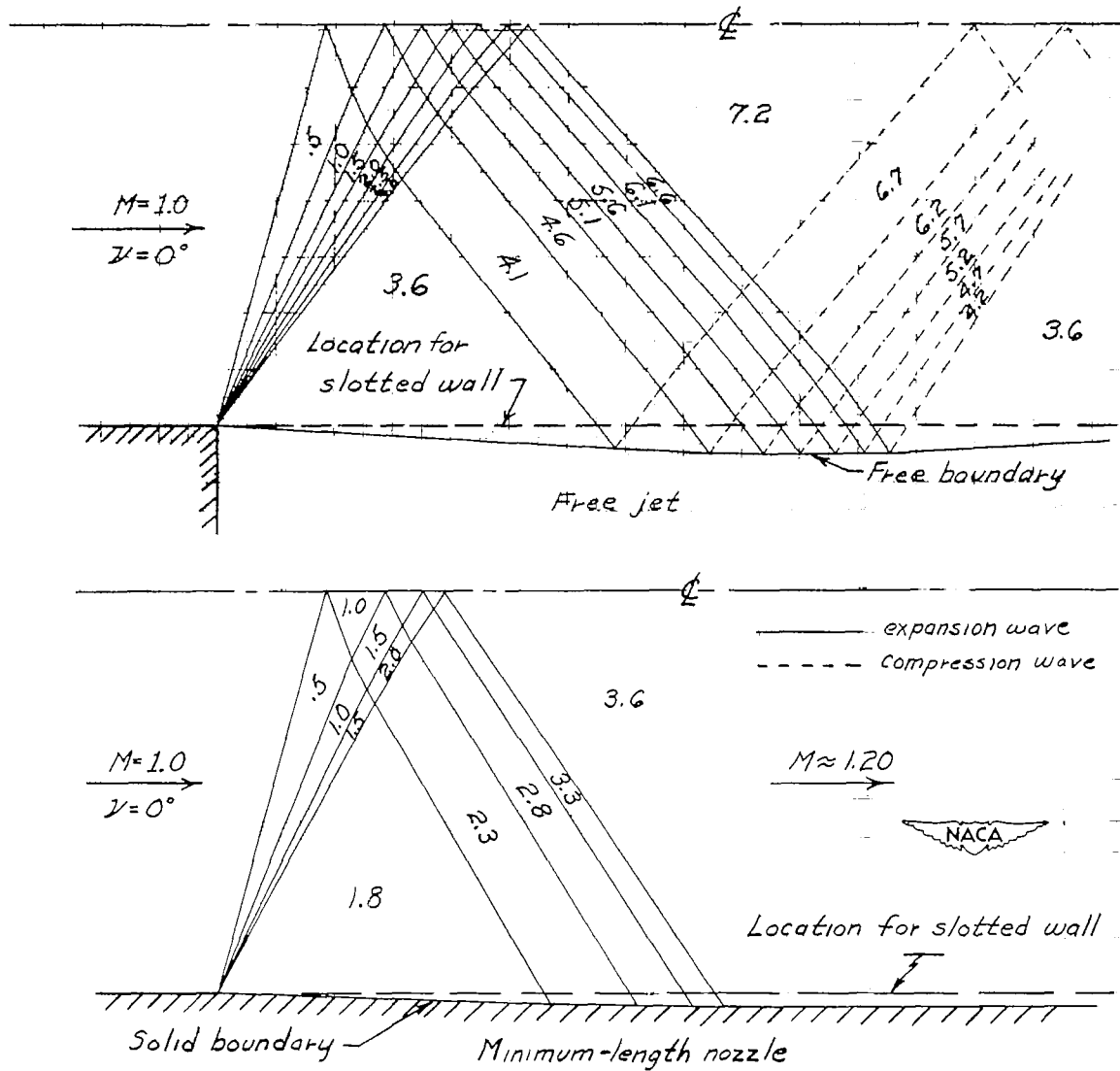
(a) $nw_B/w = 1/8$; $w_B = 0.141$ inch; $n = 4$; $\phi = 2.75^\circ$.

Figure 6.- Pressure distribution along center line; $w = 4\frac{1}{2}$ inches;
 $h = 4\frac{1}{2}$ inches.



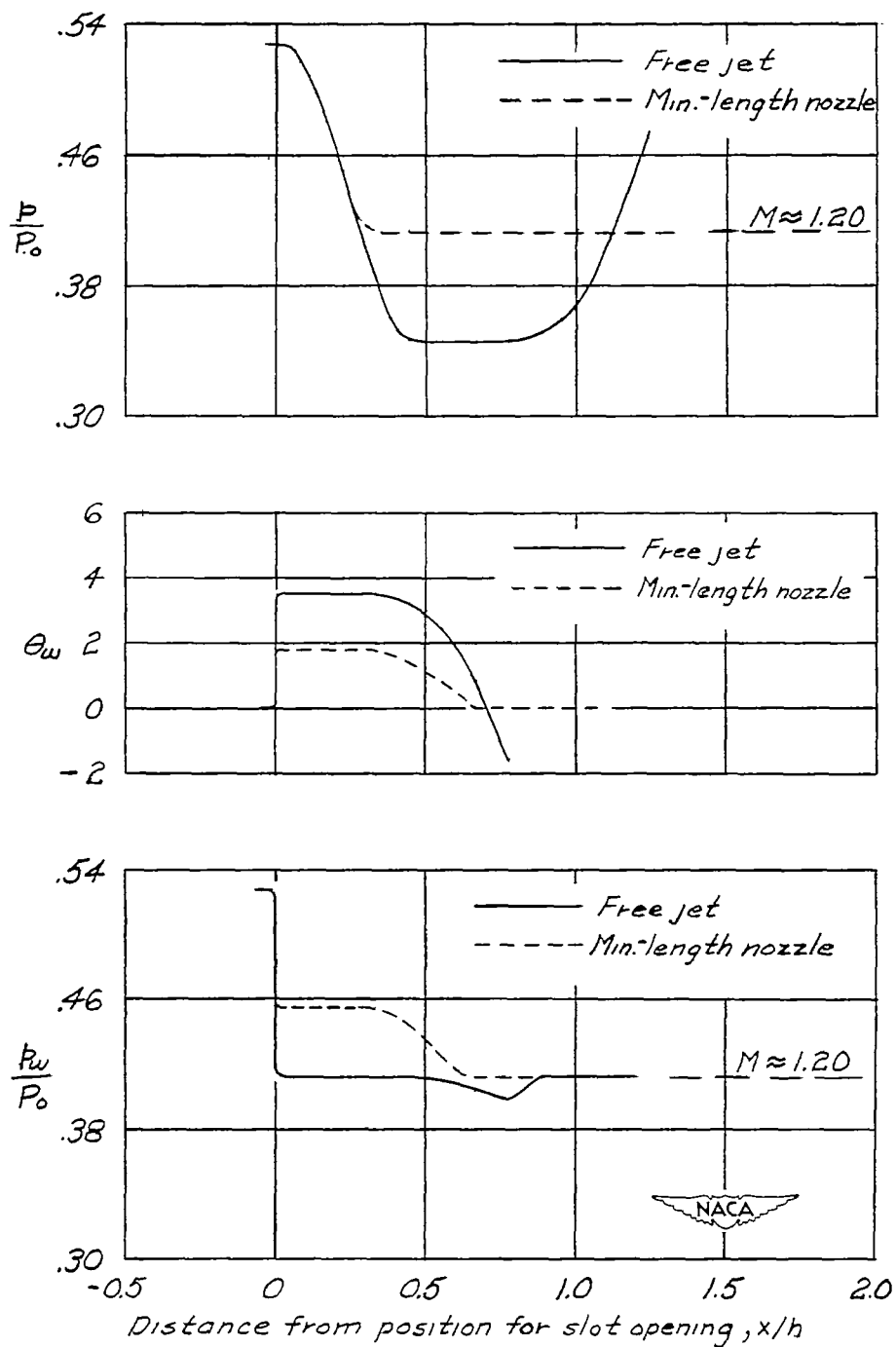
(b) $nw_B/w = 1/8$; $w_B = 0.141$ inch; $n = 4$;
 d_B , variable along taper; $\phi = 2.75^\circ$.

Figure 6.- Concluded.



(a) Characteristic nets for a free jet and minimum-length nozzle at $M \approx 1.20$.

Figure 7.- Analysis of free jet and minimum-length nozzle at $M \approx 1.20$.



(b) Calculated center-line pressure distribution and pressure and flow-angle distribution along plane parallel to the axis and passing through the edge of a free jet and a minimum-length nozzle.

Figure 7.- Concluded.

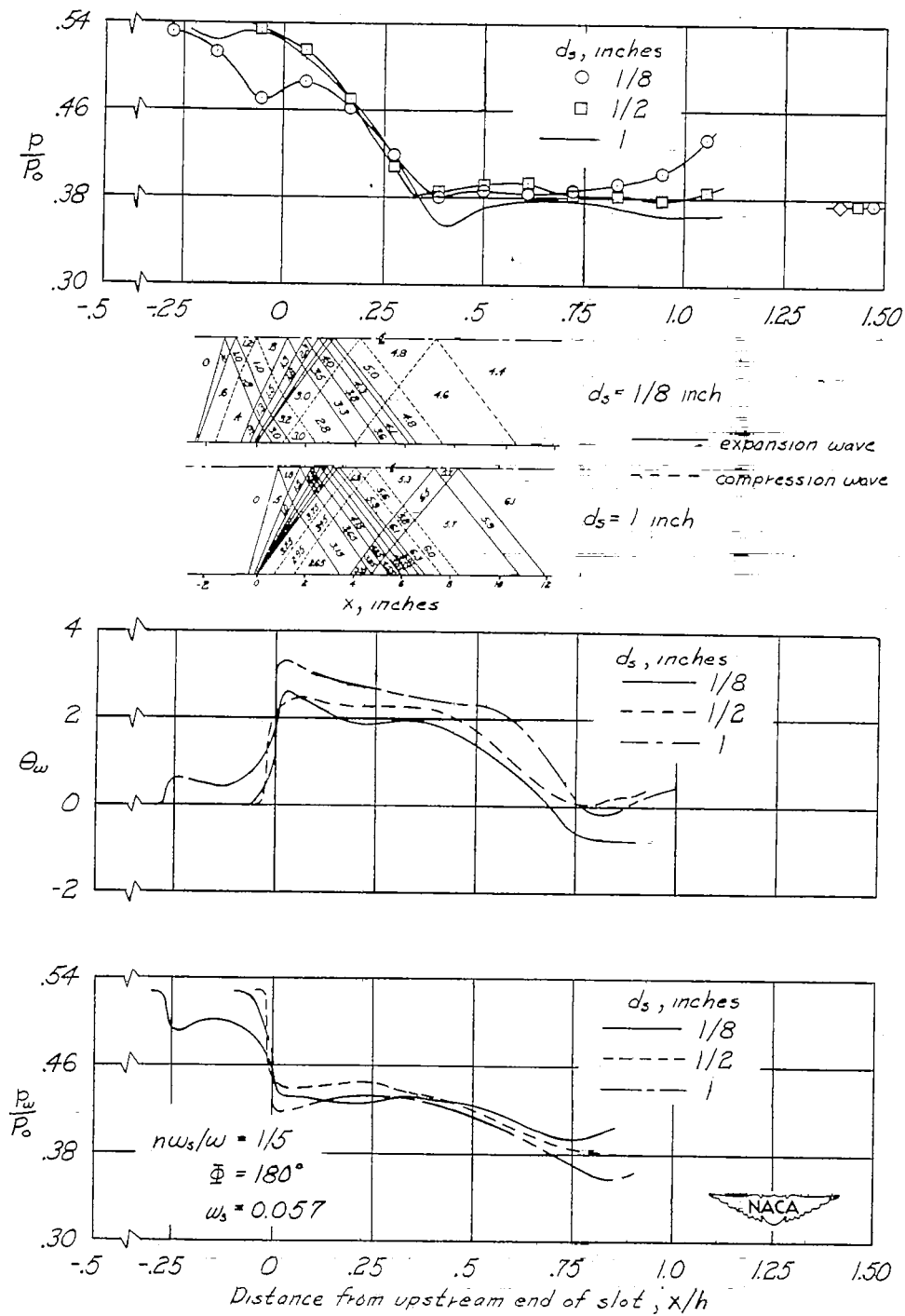
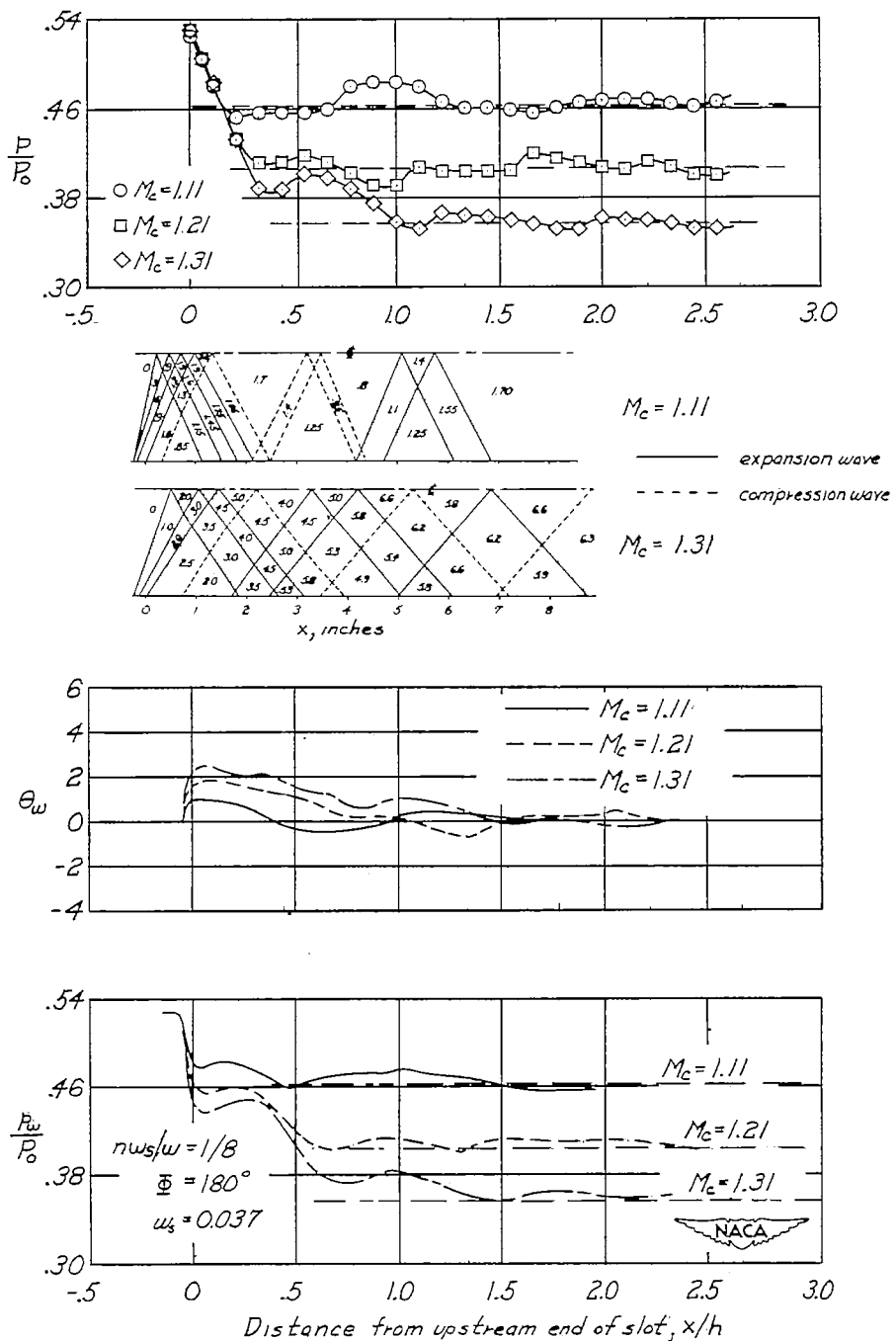
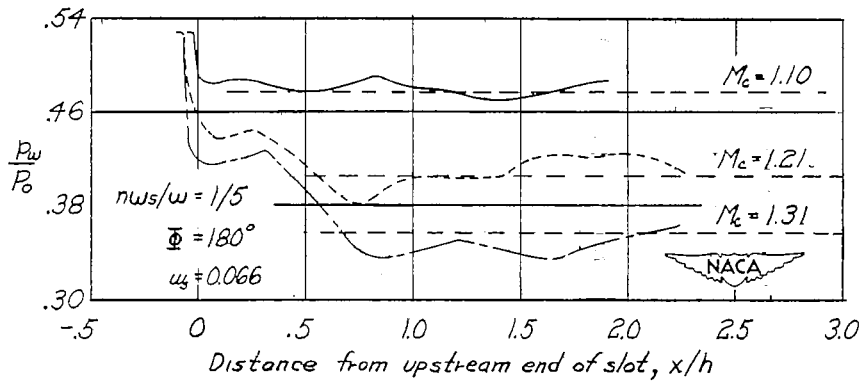
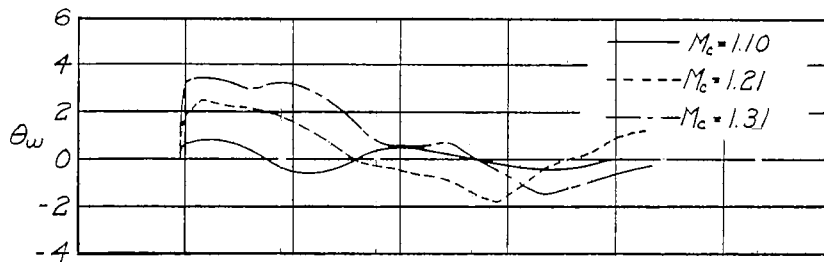
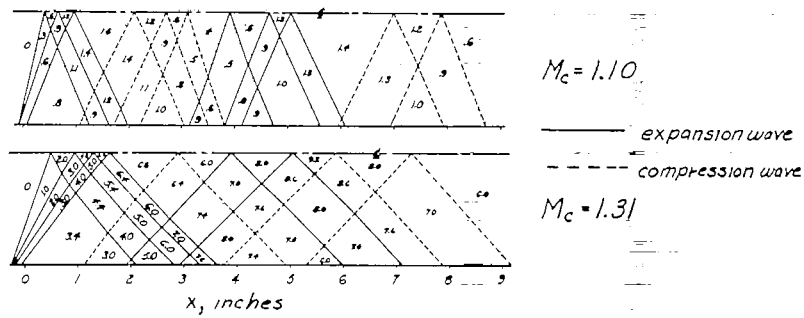
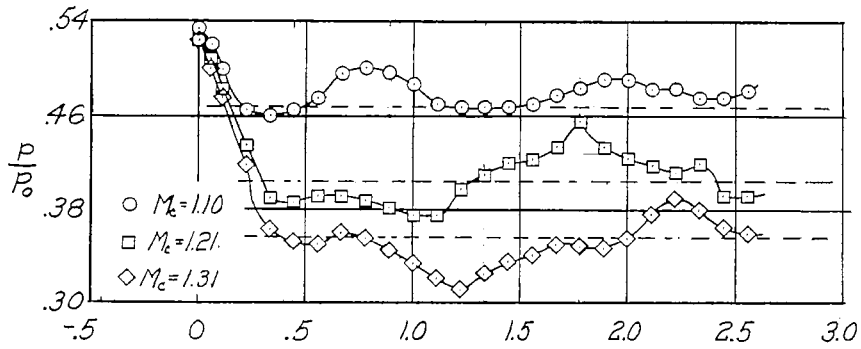


Figure 8.- Pressure and flow-angle distributions at $M \approx 1.27$;
 $w = 2\frac{1}{4}$ inches; $h = 9$ inches; $n w_s/w = 1/5$; $w_s = 0.057$ inch;
 $n = 7$; $\Phi = 180^\circ$.



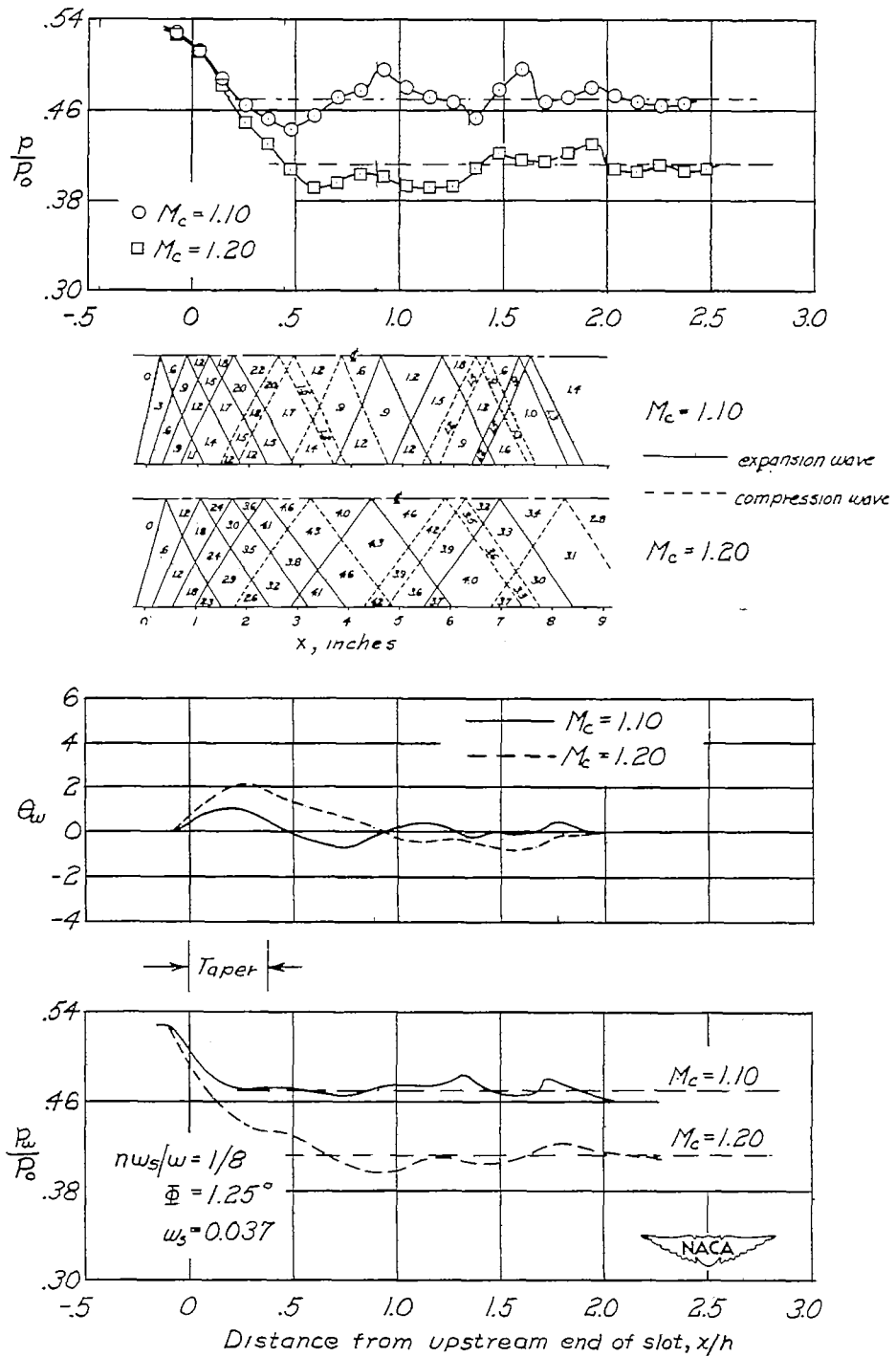
(a) $n w_s/w = 1/8$; $w_s = 0.037$ inch; $n = 21$; $\phi = 180^\circ$.

Figure 9.- Pressure and flow-angle distributions; $w = 6\frac{1}{4}$ inches;
 $h = 4\frac{1}{2}$ inches.



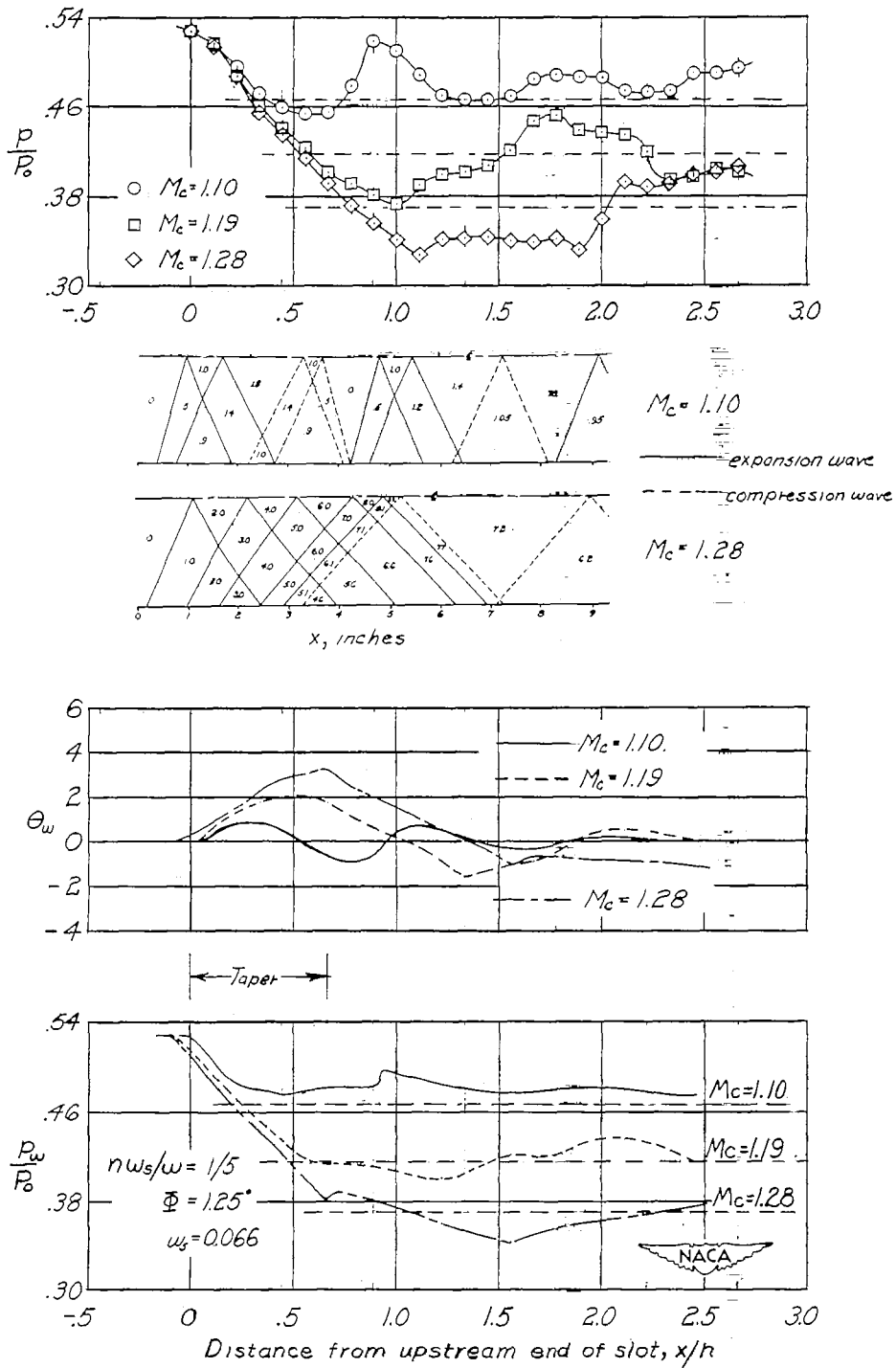
(b) $nw_s/w = 1/5$; $w_B = 0.066$ inch; $n = 19$; $\phi = 180^\circ$.

Figure 9.- Continued.



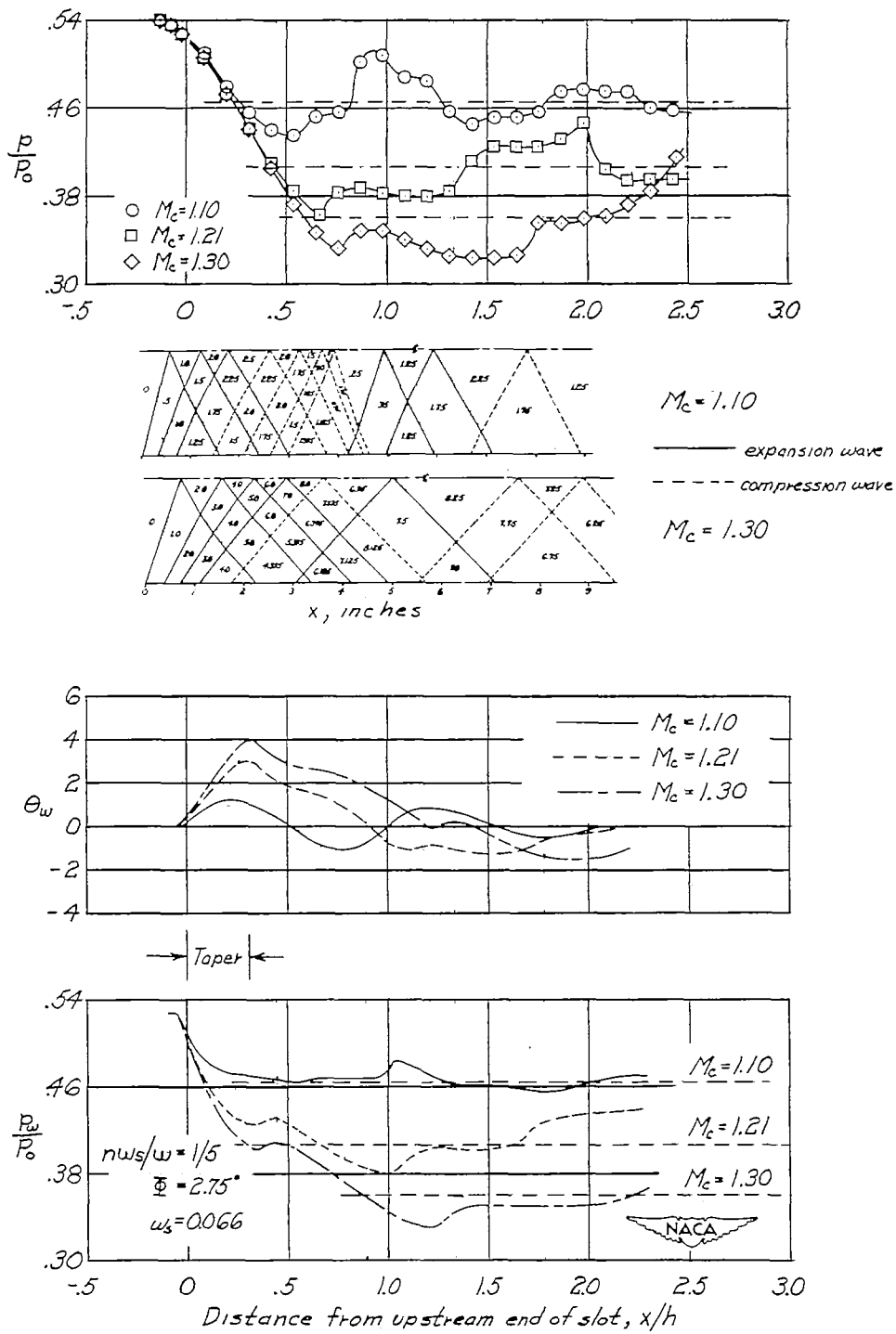
(c) $n w_s / w = 1/8$; $w_s = 0.037$ inch; $n = 21$; $\phi = 1.25^\circ$.

Figure 9.- Continued.



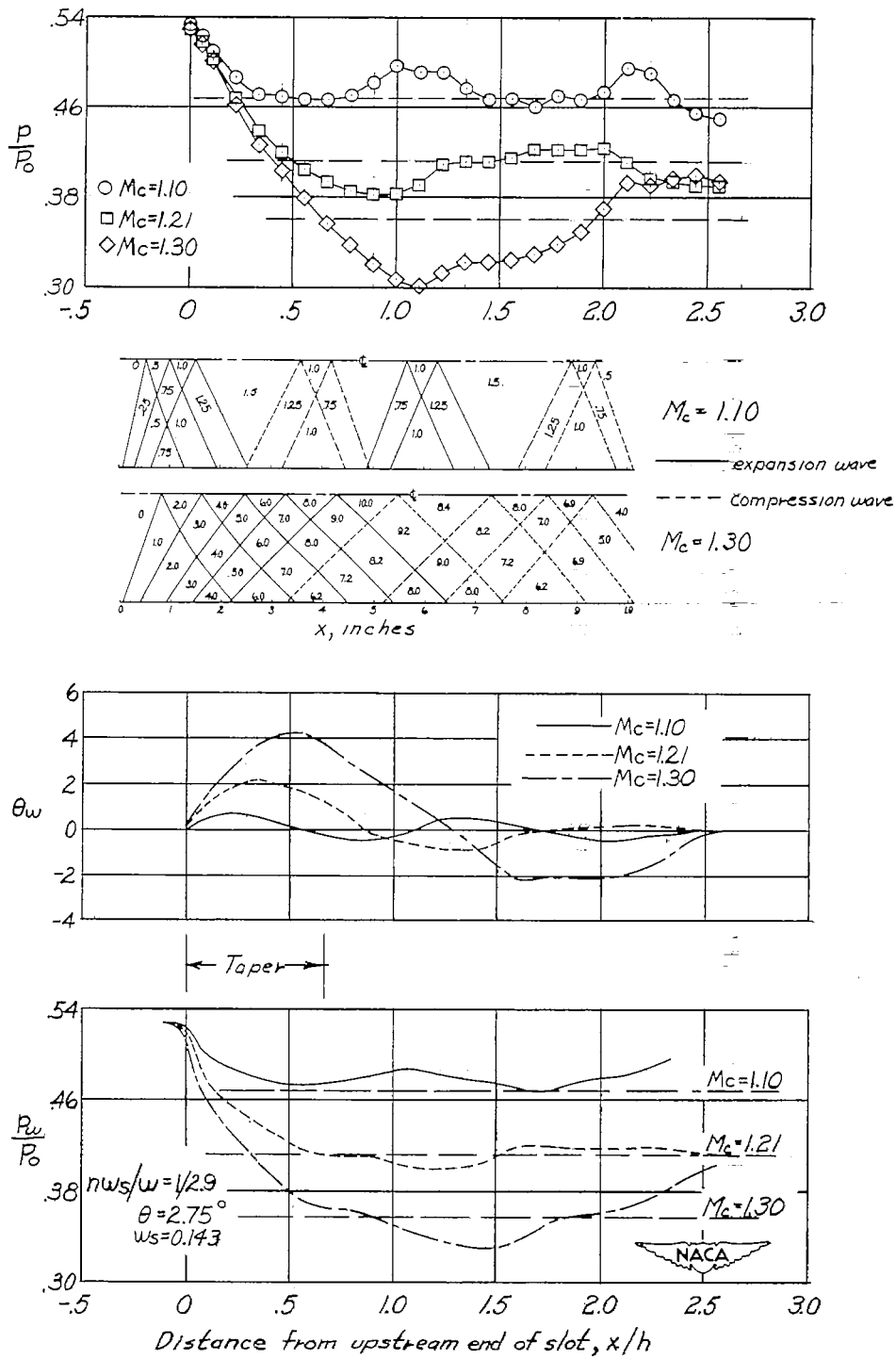
(d) $nw_s/w = 1/5$; $w_s = 0.066$ inch; $n = 19$; $\Phi = 1.25^\circ$.

Figure 9.- Continued.



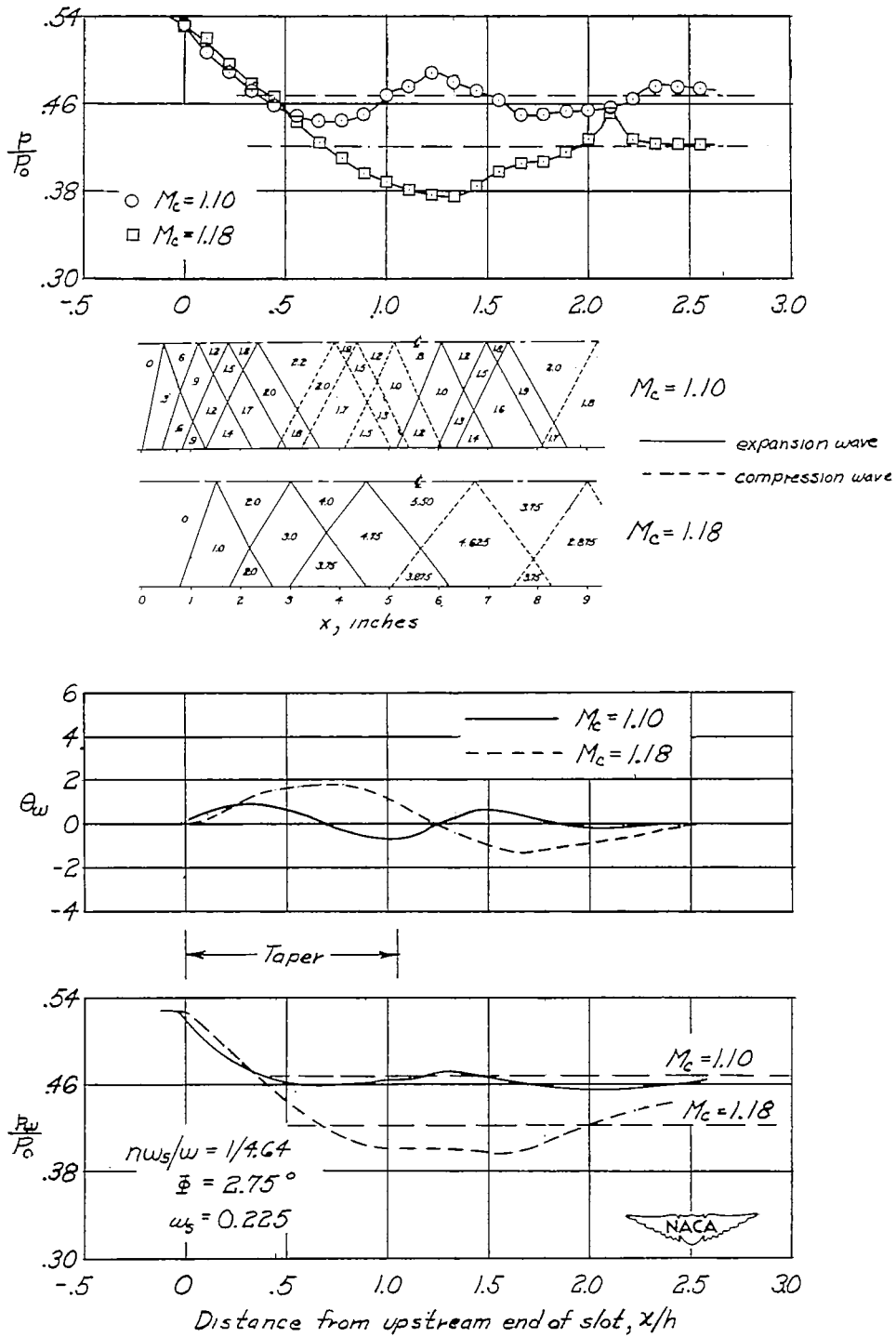
(e) $nw_s/w = 1/5$; $w_s = 0.066$ inch; $n = 19$; $\Phi = 2.75^\circ$.

Figure 9.- Continued.



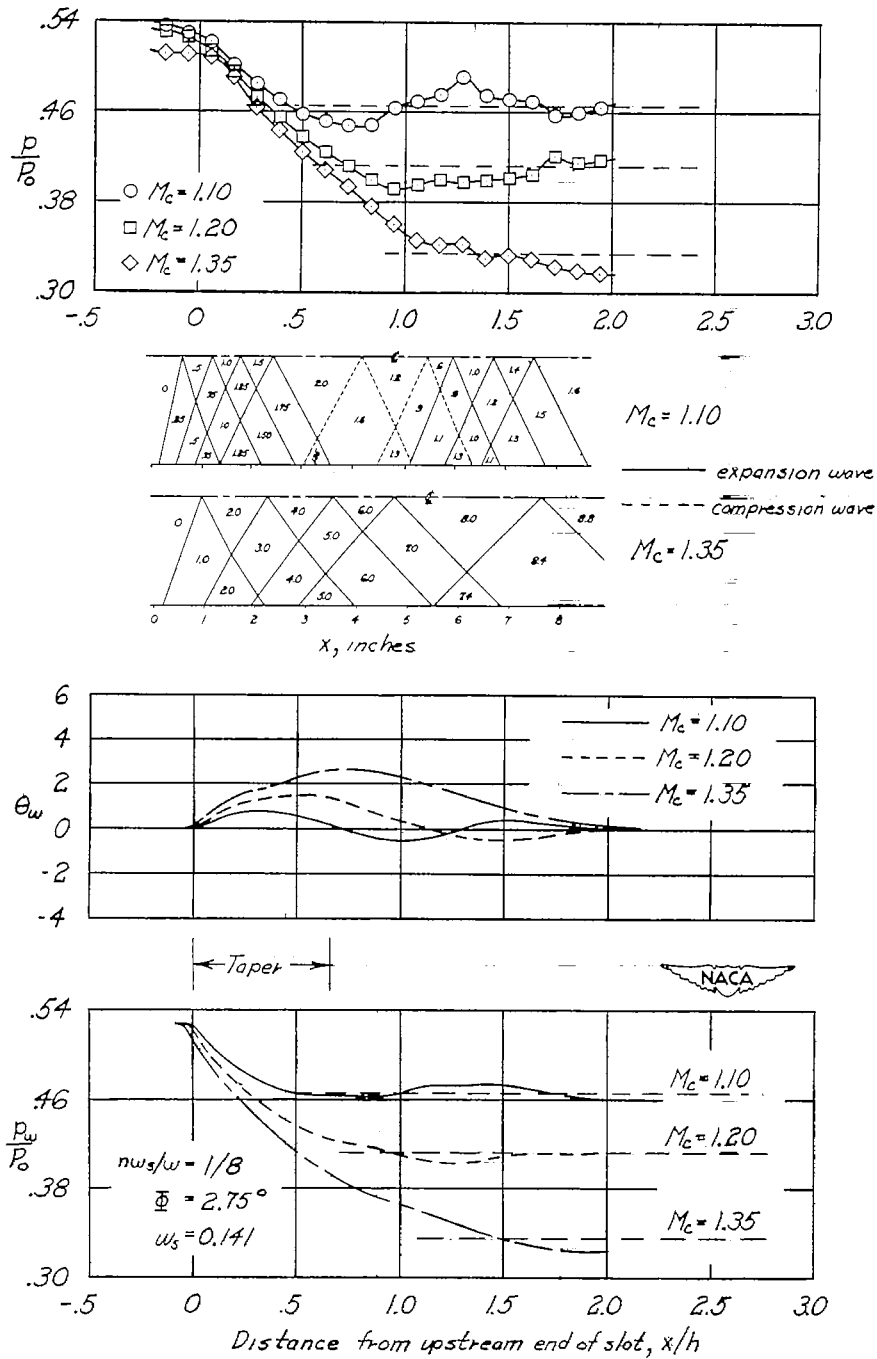
(f) $nw_s/w = 1/2.9$; $w_s = 0.143$ inch; $n = 15$; $\phi = 2.75^\circ$.

Figure 9.- Continued.



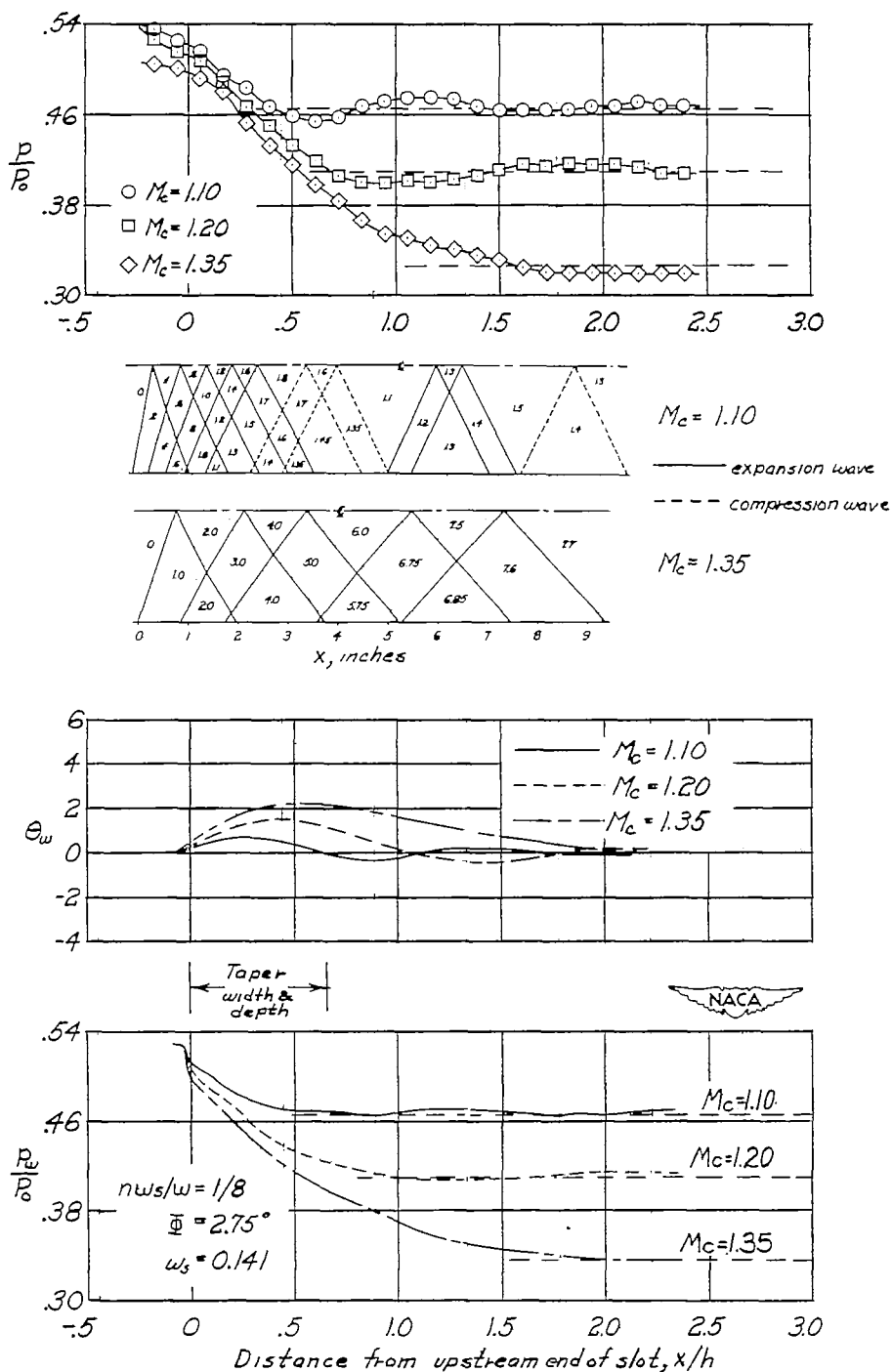
(g) $nw_s/w = 1/4.64$; $w_s = 0.225$ inch; $n = 6$; $\Phi = 2.75^\circ$.

Figure 9.- Concluded.



(a) $nw_s/w = 1/8$; $w_s = 0.141$ inch; $n = 4$; $\phi = 2.75^\circ$.

Figure 10.- Pressure and flow-angle distributions; $w = 4\frac{1}{2}$ inches;
 $h = 4\frac{1}{2}$ inches.



(b) $nw_s/w = 1/8$; $w_s = 0.141$ inch; $n = 4$;
 d_s , variable along taper; $\Phi = 2.75^\circ$.

Figure 10.- Concluded.